J. Fluid Mech. (1999), *vol.* 396, *pp.* 143–182. Printed in the United Kingdom

Reflection of oblique waves by currents: analytical solutions and their application to numerical computations

By JINN-HWA SHYU[1] AND CHI-CHAO TUNG[2]

[1] Institute of Harbor and Marine Technology, Wuchi, Taichung District, Taiwan, ROC

[2] Department of Civil Engineering, North Carolina State University, Raleigh, NC 27695, USA

(Received 2 June 1998 and in revised form 2 May 1999)

Surface waves superimposed upon a larger-scale flow are blocked and reflected at the points where the group velocities balance the convection by the larger-scale flow. In this study, we first extended the theory of Shyu & Phillips (1990) to the situation when short deep-water gravity waves propagate obliquely upon a steady unidirectional irrotational current and are reflected by it. In this case, the uniformly valid solution and the WKBJ solution of the short waves were derived from the Laplace equation and the kinematical and dynamical boundary conditions. These solutions in terms of some parameters (the expressions for which have also been deduced in this case) take the same forms as those derived by Shyu & Phillips, which by referring to Smith's (1975) theory can even be proved to be valid for gravity waves in an intermediate-depth region and near a curved moving caustic induced by an unsteady multidirectional irrotational current. In this general case, the expressions for certain parameters in these solutions cannot be obtained so that their values must be estimated in a numerical calculation. The algorithm for estimates of some of these parameters that are responsible for the amplitude of the reflected wave not being equal to that of the incident wave in the vicinity of the caustic and therefore are crucial for the computer calculation of the ray solution to be continued after reflection, was illustrated through numerical tests. This algorithm can avoid the error magnification phenomenon that occurred in the previous estimates of the reflected wave in the vicinity of the caustic using the action conservation principle directly. The forms of the solutions have also been utilized to clarify the wave profiles near caustics in a general situation, which indicate that in storm conditions freak waves characterized by a steeper forward face preceded by a deep trough will probably occur in the caustic regions.

1. Introduction

The modulation and reflection of short surface waves by a variable current or a long wave are of importance for predication of the wave fields in regions with strong non-uniform currents (see, for example, Peregrine 1976; Smith 1976; Mei 1983; Holthuijsen & Tolman 1991), and for interpretation of remote sensing records (see Phillips 1988 for a review). Modern theories on the dynamics of short waves on larger-scale currents were begun by Longuet-Higgins & Stewart (1960, 1961), Whitham (1965), and Bretherton & Garrett (1968) (see Peregrine 1976 for a review of these theories and many other developments on this subject), in which the idea of radiation stress was introduced and the action conservation equation established so that the evolution of the short waves can be determined rigorously until a caustic is met, at which these theories characteristic of a ray description all predict a singularity in the wave height and therefore are not applicable here.

The short waves blocked at the caustic will be reflected at a different wavelength, which leads to a more drastic change of wave slopes. Therefore it is important to determine the amplitude of the reflected wave in terms of that of the incident wave in the vicinity of the caustic which permits the ray solution to be continued after reflection. To achieve this goal and other scientific purposes, Smith (1975) derived a uniform asymptotic solution of short surface gravity waves near a curved moving caustic induced by an unsteady multidirectional irrotational current. This solution can be expressed as

$$u = \left\{ A\,\mathrm{Ai}\,(\rho) + \mathrm{i}C\,\mathrm{Ai}'\,(\rho) \right\} \exp\,(\mathrm{i}s) \tag{1.1}$$

with

$$\left. \begin{aligned} \rho &= -\left[\tfrac{3}{4}(\chi_1 - \chi_2)\right]^{2/3}, \quad s = \tfrac{1}{2}(\chi_1 + \chi_2), \\ A &= \pi^{1/2}(-\rho)^{1/4}(a_1 + a_2), \quad C = \pi^{1/2}(-\rho)^{-1/4}(a_1 - a_2), \end{aligned} \right\} \tag{1.2}$$

where u denotes any instantaneous property of the waves, $\mathrm{Ai}\,(\rho)$ and $\mathrm{Ai}'\,(\rho)$ represent respectively the Airy function and its derivative, and a_1, a_2, χ_1 and χ_2 correspond to the local amplitudes and phases of the incident and reflected waves which even near the caustic have been proved by Smith (1975) to fulfil the action conservation equation and the local dispersion relation. The above unified formulae were summarized by Peregrine & Smith (1979).

In (1.2), the requirement that C remains finite and analytic at caustics implies that a_1 and a_2 have equal singularities there. This, together with the action conservation equation 'enables us to conclude that the flux of wave action normal to the caustic carried by the incident and by the reflected waves are equal and opposite' (Smith 1975). Thus, near the caustic, the amplitude of the reflected wave relative to that of the incident wave can be determined in theory. However, in the immediate vicinity of the caustic, the amplitude a_1 of the incident wave itself cannot be solved accurately from the action conservation equation by using any numerical method (ray-tracing or gridded method), because of the singularity of a_1 (and χ_1) at the caustic. At a certain distance from the caustic, the numerical solution of a_1 becomes reliable and the difference between a_1 and a_2, though small, is not negligible. Therefore an effort can be made to estimate a_2, and from the action conservation principle, we have in these regions,

$$(U_x + C_{gx2})\frac{a_2^2}{\sigma_2} = -(U_x + C_{gx1})\frac{a_1^2}{\sigma_1} + \cdots, \tag{1.3}$$

where σ_1 and σ_2 are the intrinsic frequencies of the incident and reflected waves, U_x and C_{gx} the x-components of the local current and group velocities, and the x-axis (which might be curvilinear) is perpendicular to the caustic. In (1.3) the extra terms denoted by dots (the contents of which will become clear in § 7) are small compared with each of the two terms shown explicitly, but otherwise are not negligible in a general situation in which the divergence of the action flux in the y-direction or the local rate of change of wave action is significant. From (1.3) it follows that

$$\frac{a_2}{a_1} = \left[-\frac{(U_x + C_{gx1})/\sigma_1}{(U_x + C_{gx2})/\sigma_2} \right]^{1/2} + \cdots = 1 + \varepsilon, \tag{1.4}$$

in which ε again represents a small quantity, because

$$(U_x + C_{gx1})/\sigma_1 \approx -(U_x + C_{gx2})/\sigma_2$$

in these regions. The relation (1.4) permits us, in theory, to determine the amplitude of the reflected wave in terms of that of the incident wave in the vicinity of the caustic. However, since for both incident and reflected waves, $U_x + C_{gx} = 0$ at the caustic, we have

$$|U_x + C_{gx1}| \ll |U_y + C_{gy1}|, \qquad |U_x + C_{gx2}| \ll |U_y + C_{gy2}|, \tag{1.5}$$

not too far from the caustic provided that the components of action fluxes in the y-direction are significant, which often occurs in the situation when the waves and currents are not collinear. Consequently, slight misalignment of the coordinate lines can cause large changes in U_x+C_{gx1} and U_x+C_{gx2} in opposite directions, that will produce an even larger percent change in ε in (1.4), because $\varepsilon \ll 1$. Therefore a very serious error magnification phenomenon will occur in the estimates of the difference between a_1 and a_2 in these regions in a general situation if the action conservation principle is utilized directly. This phenomenon will certainly become less severe far away from the caustic, but in these regions the values of a_2/a_1 in general cannot be determined without knowledge of a_2 itself, because here the first term in the asymptotic expansion of the parameter ε in (1.4), which can be estimated without knowing a_2, will become invalid. Therefore it is of practical importance to develop another theory for estimates of a_2/a_1 in the vicinity of the caustic that can avoid the error magnification phenomenon.

The blockage and reflection of short waves by currents or long waves can also occur for capillary waves with opposite characteristics as suggested by Phillips (1981). The uniformly valid solutions of this capillary blockage phenomenon were given by Shyu & Phillips (1990) and by Trulsen & Mei (1993) who even derived a uniform solution near a triple turning point at which the two kinds of reflection points coalesce to one. In these two theories, the expressions for a_1 and a_2 take an explicit form instead of being described by the action conservation equation or its equivalent, but these analyses were restricted to the case when both the wave and current are unidirectional and are in the same or opposite directions. (Shyu & Phillips' 1990 theory also requires that the underlying current is steady in a moving frame of reference.) Thus an extension of the theories to a more general situation is desired for practical applications.

In this paper we shall extend Shyu & Phillips' (1990) theory first to the case when short deep-water gravity waves propagate obliquely upon a steady unidirectional irrotational current. In this case, a second-order ordinary differential equation for the surface displacement η of the short waves is again deduced from the Laplace equation and the kinematical and dynamical boundary conditions, which can be written as

$$\frac{\partial^2 \eta}{\partial x^2} + [-\mathrm{i}(k_{x1} + k_{x2}) + Q]\frac{\partial \eta}{\partial x} + [-k_{x1}k_{x2} + P]\eta = 0. \tag{1.6}$$

The similarity between the forms of this equation and equation (6.3) in Shyu & Phillips (1990) is remarkable, although the wavenumbers k_1 and k_2 of the incident and reflected waves in the latter are replaced respectively by their x-components k_{x1} and k_{x2} in (1.6) due to the fact that k_1 and k_2 in the present case also contain k_{y1} and k_{y2} respectively, which are irrelevant to the rapid variation of η in the x-direction.

The terms in the coefficients of (1.6) and in many other equations derived below can be divided into two classes. The Class 1 terms, such as $-\mathrm{i}(k_{x1} + k_{x2})$ and $-k_{x1}k_{x2}$ in (1.6), involve the slowly varying parameters representing the local properties of the wave trains and current but not the rates of change of these properties which will vanish if the current field (and therefore the wave trains) is uniform. On the other hand, the Class 2 terms, such as those designated by P and Q in (1.6), are characterized by a linear combination (the case that only one term exists included) of the first derivatives of the above-mentioned parameters. Therefore, when the underlying current field is slowly varying so that the local properties of the wave trains will similarly vary slowly, the Class 2 terms are always smaller than the Class 1 terms in the same equation. This situation can be best seen from Shyu & Phillips' (1990) equation (6.3), in which $P = -2\mathrm{i}(n_0/U^2)(\partial U/\partial x)$ (where n_0 is the observed frequency of both the incident and reflected waves) so that $P = O((n_0/U^2)(\partial U/\partial x)) = O((k_1/U)(\partial U/\partial x),\ (k_2/U)(\partial U/\partial x)) \ll k_1k_2$ according to the definition of a slowly varying current field (the relation $n_0 = O(Uk_1, Uk_2)$ invoked here can be inferred from the relation $n_0 = \sigma + Uk = 2C_gk + Uk$ and from the fact that the current speed has the same order of magnitude as the group velocities in the vicinity of the caustic). Note that in the more traditional perturbation scheme which is of wider application, the Class 2 terms would appear as the secular terms in the second equation in the hierarchy arising from an asymptotic expansion. Nevertheless, in this expansion the second-order solution will become unbounded unless conditions are imposed on the secular terms in the second equation which lead to the further equation for the first-order solution (see, for example, Whitham 1974 and Mei 1983). Therefore the Class 2 terms, though smaller, are not negligible even for determination of the first-order solution only.

The expressions for P and Q in the present case are much more complicated than those in Shyu & Phillips (1990), but still their regularities and those of $-\mathrm{i}(k_{x1} + k_{x2})$ and $-k_{x1}k_{x2}$ at the caustic will be shown in § 4. Therefore equation (1.6) is regular at the caustic and its uniform asymptotic solution and the corresponding WKBJ solution are derived in § 5, which in terms of the parameters again take the same forms as those in Shyu & Phillips (1990). All of these similarities lead us to hope that even for waves in an intermediate-depth region and near a curved moving caustic induced by an unsteady multidirectional irrotational current, the forms of the equation and therefore the solutions may still be the same. This anticipation, especially the regularities of the resulting equation and its uniform solution at the caustic, will in § 6 be verified through considerations of the dispersion relation and the action conservation equation, the validity of which in the vicinity of the caustic has been demonstrated by Smith (1975) in exactly the same circumstances.

In this general situation, the expressions for the Class 2 terms in the solutions cannot be obtained, though their Taylor series expansions about the caustic are proved to exist in § 6. Since some of these Class 2 terms are responsible for a_2 being not equal to a_1 in the vicinity of the caustic, the estimate of these Class 2 terms in this region in a numerical computation is crucial for determination of a_2 in terms of a_1 in the same region, which will permit the computer calculation of the ray solution to be continued after reflection. The algorithm for estimates of these Class 2 terms is developed and tested in § 7 through numerical simulations of a straight caustic (encountered by oblique waves) and a curved caustic, but its validity in the case of a moving caustic is also obvious. In this algorithm, by taking advantage of the explicit forms of the expressions for a_1 and a_2 in the present WKBJ solution, the aforementioned error magnification phenomenon can mostly be avoided. These estimates still represent an asymptotic approximation so that their accuracy is examined through a comparison between the analytical and numerical solutions in the case of a straight caustic in which the expressions for the Class 2 terms exist.

The present solutions for the case of a straight caustic can also be utilized to advantage in determination of every detail of the wave profiles in the vicinity of the caustic, after which it becomes clear that the chief features of these estimate profiles can be attributed to the specific forms of the solutions and to the characteristics of their parameters, which are all valid for the case of a curved moving caustic too. These chief features, in storm conditions, though subject to modification by the nonlinear effects, coincide with those of freak waves which according to Mallory (1974) have a steeper forward face preceded by a deep trough, or 'hole in the sea' (White & Fornberg 1998). Therefore the situation where freak waves (which are different from extreme waves investigated theoretically by Phillips, Gu & Donelan 1993*a* and observationally by Phillips, Gu & Walsh 1993*b*) are produced in the caustic regions, suggested first by Peregrine (1976) and Smith (1976), is illuminated in § 8.

2. The ordinary differential equation for a single wave component

In this section we shall derive an ordinary differential equation for short deep-water gravity waves propagating obliquely on a steady unidirectional irrotational current $U(x)\boldsymbol{i}$ where $\boldsymbol{i}$ denotes the unit vector in the direction of increase of x. For gravity–capillary waves propagating in the direction parallel to this current, Shyu & Phillips (1990) have derived a third-order ordinary differential equation (see their (2.19)) in the surface displacement η of the short waves. This equation was then decomposed into a second-order ordinary differential equation in which all the coefficients are regular at the caustic so that a uniformly valid solution of the short waves subject to reflection by currents can be obtained. This approach was successful because in this case expansion of the dispersion relation

$$n = (g'k + \gamma k^3)^{1/2} + Uk \tag{2.1}$$

takes the form

$$k^3 - \frac{U^2}{\gamma}k^2 + \frac{g' + 2nU}{\gamma}k - \frac{n^2}{\gamma} = 0,$$

which is a third-order polynomial equation in k and its coefficients are the same as the Class 1 coefficients of the above-mentioned third-order differential equation (this equivalence will become even clearer if we define $\lambda \equiv \mathrm{i}k$ and rewrite the above equation in terms of λ). In (2.1), g' is the effective gravitational acceleration suggested by Phillips (1981), n the observed frequency of the wave, and γ the ratio of surface tension to water density.

When the waves propagate obliquely upon the current and the effects of surface tension are neglected, the dispersion relation becomes

$$n = \left[g(k_x^2 + k_y^2)^{1/2}\right]^{1/2} + Uk_x, \tag{2.2}$$

if the x-axis is chosen to be exactly opposite to the current (so that in (2.2) U is always negative). Notice that if the slope and curvature of the mean free surface becomes significant, the x-axis (and the y-axis) along the mean free surface is also curved and the gravitational acceleration g in (2.2) should be replaced by g' according to Phillips (1981), Longuet-Higgins (1985, 1987) and Henyey *et al.* (1988). An expansion of (2.2) yields

$$U^4k_x^4 - 4nU^3k_x^3 + (6n^2U^2 - g^2)k_x^2 - 4n^3Uk_x + (n^4 - g^2k_y^2) = 0, \tag{2.3}$$

which is a quartic equation. From it and from Shyu & Phillips (1990) analysis, it is anticipated that a fourth-order ordinary differential equation is needed in order to eventually obtain a second-order equation by decomposition that can describe the reflection phenomenon as well as be uniformly valid.

To obtain this fourth-order equation, certain results of the ray theory will be utilized. It is invalid in the immediate vicinity of the caustic, but as long as we can prove that the resulting second-order differential equation is regular at this point (meaning that the singularities inherent in the ray solutions of the incident and reflected waves are completely offset from this equation), this equation can be applicable virtually everywhere, including the caustic.

Also we emphasize that both the uniformly valid solution and the ray solution represent the first-order approximations of asymptotic expansions, and in these expansions each differentiation of the slowly varying parameters increases the order by one (see e.g. Whitham 1974). Therefore, in the following discussion in which a single differential equation, instead of a hierarchy of equations, is pursued, the derivatives of these parameters, except their first derivatives which are among the Class 2 terms, and the products of any two or more derivatives of these parameters can all be neglected, and if using this ordering, there is no need to introduce explicitly an ordering parameter in the analysis.

For a slowly varying wave train, the distribution of the wavenumber vector $\boldsymbol{k}$ is irrotational (see e.g. Phillips 1977) so that

$$\frac{\partial k_y}{\partial x} - \frac{\partial k_x}{\partial y} = 0. \tag{2.4}$$

On the other hand, since the current velocity is independent of y, we have

$$\frac{\partial k_x}{\partial y} = 0 \quad \text{and} \quad \frac{\partial k_y}{\partial y} = 0. \tag{2.5}$$

From (2.4) and (2.5) it immediately follows that

$$k_y = \text{constant}$$

everywhere. Next, from the kinematical conservation equation,

$$\frac{\partial \boldsymbol{k}}{\partial t} + \nabla n = 0,$$

where $\nabla \equiv (\partial/\partial x, \partial/\partial y)$ represent the horizontal gradient operator. Thus, if the current field is steady, we also have

$$n = \text{constant} = n_0,$$

say, everywhere. Therefore, the ray solutions of the surface displacement η and the velocity potential ϕ of a single wave component can now be written as

$$\eta = a(x) \exp\left[\mathrm{i} \int k_x(x)\,\mathrm{d}x\right] \exp \mathrm{i}(k_y y - n_0 t), \tag{2.6}$$

and

$$\phi = A(x) \exp\left[\mathrm{i} \int k_x(x)\,\mathrm{d}x + \int_0^z l(x,z)\,\mathrm{d}z\right] \exp \mathrm{i}(k_y y - n_0 t), \tag{2.7}$$

where $a(x), A(x)$ and $k_x(x)$ vary slowly in the x-direction and $l(x,z)$ varies slowly in both the x- and z-directions. For the sake of definiteness, we here take $z = 0$ to be the mean water level. Notice that in (2.6) and (2.7) the roles played by k_y and n_0 are quite similar.

The relation between $\boldsymbol{k}$ and l can be deduced from the three-dimensional Laplace equation

$$\left(\frac{\partial^2}{\partial x^2}+\frac{\partial^2}{\partial y^2}+\frac{\partial^2}{\partial z^2}\right)\phi=0. \tag{2.8}$$

Substitution of (2.7) into (2.8) yields

$$-k_x^2+\mathrm{i}\frac{\mathrm{d}k_x}{\mathrm{d}x}+2\mathrm{i}k_x\frac{1}{A}\frac{\mathrm{d}A}{\mathrm{d}x}-k_y^2+l^2+\frac{\partial l}{\partial z}=0 \quad \text{at } z=0, \tag{2.9}$$

in which the higher-order term $(1/A)(\mathrm{d}^2A/\mathrm{d}x^2)$ has been neglected, and the terms $\mathrm{i}(\mathrm{d}k_x/\mathrm{d}x)$, $2\mathrm{i}k_x(1/A)(\mathrm{d}A/\mathrm{d}x)$ and $\partial l/\partial z$ have been classified among the Class 2 terms, while $-k_x^2$ and $l^2-k_y^2$ represent the Class 1 terms. Considering the definition of a slowly modulated wave train and anticipating the results below for l and $\partial l/\partial z$, it can easily be seen that the Class 2 terms in (2.9) are indeed smaller than its Class 1 terms.

In (2.9), since both l and $\partial l/\partial z$ exist, we cannot express l in terms of other parameters and their derivatives without deriving another equation. To obtain such an equation, we reconsider the simpler case when the waves are exactly opposite to the current. In this case, (2.8) reduces to

$$\left(\frac{\partial^2}{\partial x^2}+\frac{\partial^2}{\partial z^2}\right)\phi=0 \tag{2.10}$$

or

$$\left(\frac{\partial}{\partial x}+\mathrm{i}\frac{\partial}{\partial z}\right)\left(\frac{\partial}{\partial x}-\mathrm{i}\frac{\partial}{\partial z}\right)\phi=0.$$

In addition, from the deep-water boundary condition and the fact that the phases of oscillation of both incident and reflected waves increase in the positive x-direction (because both k_1 and k_2 are positive), it is clear that the solution under consideration should satisfy

$$\left(\frac{\partial}{\partial x}-\mathrm{i}\frac{\partial}{\partial z}\right)\phi=0 \tag{2.11}$$

only, otherwise the part of the solution which satisfies

$$\left(\frac{\partial}{\partial x}+\mathrm{i}\frac{\partial}{\partial z}\right)\phi=0$$

will grow exponentially as $z\to-\infty$ (for a rigorous analysis which even considers the effects of a curved mean free surface, see Shyu & Phillips 1990). Substituting (2.7) into (2.10) and (2.11) and setting $k_y=0$ and $k_x=k$, we obtain at the free surface

$$-k^2+\mathrm{i}\frac{\mathrm{d}k}{\mathrm{d}x}+2\mathrm{i}k\frac{1}{A}\frac{\mathrm{d}A}{\mathrm{d}x}+l^2+\frac{\partial l}{\partial z}=0 \tag{2.12}$$

and

$$\mathrm{i}k+\frac{1}{A}\frac{\mathrm{d}A}{\mathrm{d}x}=\mathrm{i}l, \tag{2.13}$$

respectively. Squaring both sides of (2.13), neglecting the higher-order term $(1/A)^2(\mathrm{d}A/\mathrm{d}x)^2$, and then subtracting the result from (2.12), we obtain

$$\left.\frac{\partial l}{\partial z}\right|_{z=0}=-\mathrm{i}\frac{\mathrm{d}k}{\mathrm{d}x}. \tag{2.14}$$

The above relation involves only the Class 2 terms so that when the waves propagate obliquely upon a unidirectional current, and if at each point a local coordinate system (x', y') is under consideration in which the x'-axis is perpendicular to the local wave crest, the small curvature of the wave crest induced in this case will impose a modification of (2.14) smaller than the Class 2 terms, which is certainly negligible within the present approximation. Therefore, in this case, we still have

$$\left.\frac{\partial l}{\partial z}\right|_{z=0} = -\mathrm{i}\frac{\partial k}{\partial x'},$$

where $k = (k_x^2 + k_y^2)^{1/2}$ represents the magnitude of $\boldsymbol{k}$. In the present coordinate system this can be written as

$$\left.\frac{\partial l}{\partial z}\right|_{z=0} = -\mathrm{i}\frac{k_x^2}{k^2}\frac{\mathrm{d}k_x}{\mathrm{d}x}, \tag{2.15}$$

because k_y = constant and k_x is independent of y. Substitution in (2.9) yields

$$\left. l^2\right|_{z=0} = k^2 - 2\mathrm{i}k_x\frac{1}{A}\frac{\mathrm{d}A}{\mathrm{d}x} - \mathrm{i}\left(1 - \frac{k_x^2}{k^2}\right)\frac{\mathrm{d}k_x}{\mathrm{d}x},$$

and its square root is

$$\left. l\right|_{z=0} = k - \mathrm{i}\frac{k_x}{k}\frac{A'}{A} - \frac{\mathrm{i}}{2}\left(1 - \frac{k_x^2}{k^2}\right)\frac{k_x'}{k} \tag{2.16}$$

within the present approximation. (Here, and for the rest of the paper, we use a prime to indicate differentiation with respect to x in certain circumstances.) Notice that (2.16) can be reduced to (2.13) when $k_y = 0$.

From (2.7) and (2.16) and neglecting the higher-order terms, one can obtain at $z = 0$

$$\frac{\partial \phi}{\partial x} = \mathrm{i}\frac{k_x}{k}\left[1 - \mathrm{i}c_0\frac{A'}{A} + \mathrm{i}c_1 k_x'\right]\frac{\partial \phi}{\partial z}, \tag{2.17a}$$

$$\frac{\partial^2 \phi}{\partial x^2} = \mathrm{i}\frac{k_x}{k}\left[1 - \mathrm{i}c_0\frac{A'}{A} + \mathrm{i}c_2 k_x'\right]\frac{\partial^2 \phi}{\partial x \partial z}, \tag{2.17b}$$

$$\frac{\partial^3 \phi}{\partial x^3} = \mathrm{i}\frac{k_x}{k}\left[1 - \mathrm{i}c_0\frac{A'}{A} + \mathrm{i}c_3 k_x'\right]\frac{\partial^3 \phi}{\partial x^2 \partial z}, \tag{2.17c}$$

$$\frac{\partial^4 \phi}{\partial x^4} = \mathrm{i}\frac{k_x}{k}\left[1 - \mathrm{i}c_0\frac{A'}{A} + \mathrm{i}c_4 k_x'\right]\frac{\partial^4 \phi}{\partial x^3 \partial z}, \tag{2.17d}$$

where

$$\left.\begin{array}{l} c_0 = \dfrac{1}{k_x}\left(1 - \dfrac{k_x^2}{k^2}\right), \quad c_1 = \dfrac{1}{2k^2}\left(1 - \dfrac{k_x^2}{k^2}\right), \quad c_2 = -\dfrac{1}{k_x^2}\left(1 - \dfrac{3}{2}\dfrac{k_x^2}{k^2} + \dfrac{1}{2}\dfrac{k_x^4}{k^4}\right), \\ c_3 = -\dfrac{1}{k_x^2}\left(2 - \dfrac{5}{2}\dfrac{k_x^2}{k^2} + \dfrac{1}{2}\dfrac{k_x^4}{k^4}\right), \quad c_4 = -\dfrac{1}{k_x^2}\left(3 - \dfrac{7}{2}\dfrac{k_x^2}{k^2} + \dfrac{1}{2}\dfrac{k_x^4}{k^4}\right). \end{array}\right\} \tag{2.17e}$$

These will later be applied to combine the two surface boundary conditions into one equation. Note that when $k_y = 0$, (2.17a) also reduces to (2.11).

Since the x-axis is taken in the direction exactly opposite to the current and the latter itself is steady and unidirectional, the expressions for the kinematic and dynamical free-surface conditions in the present case take exactly the same form as those derived in Shyu & Phillips (1990), which when $\gamma = 0$ are

$$-\mathrm{i}n_0\eta + U\eta' + \eta U' = \frac{\partial \phi}{\partial z} \quad \text{at } z = 0, \tag{2.18}$$

$$-\mathrm{i}n_0\phi + g\eta + U\frac{\partial \phi}{\partial x} = 0 \quad \text{at } z = 0. \tag{2.19}$$

These equations represent a linear wave approximation but otherwise are exact. If again the derivatives of the slowly varying parameter U with order higher than the first one are neglected, we have

$$(-\mathrm{i}n_0 + 2U')\eta' + U\eta'' = \frac{\partial^2 \phi}{\partial x \partial z}, \tag{2.20a}$$

$$(-\mathrm{i}n_0 + 3U')\eta'' + U\eta''' = \frac{\partial^3 \phi}{\partial x^2 \partial z}, \tag{2.20b}$$

$$(-\mathrm{i}n_0 + 4U')\eta''' + U\eta^{\mathrm{iv}} = \frac{\partial^4 \phi}{\partial x^3 \partial z}, \tag{2.20c}$$

from (2.18), and

$$(-\mathrm{i}n_0 + U')\frac{\partial \phi}{\partial x} + g\eta' + U\frac{\partial^2 \phi}{\partial x^2} = 0, \tag{2.21a}$$

$$(-\mathrm{i}n_0 + 2U')\frac{\partial^2 \phi}{\partial x^2} + g\eta'' + U\frac{\partial^3 \phi}{\partial x^3} = 0, \tag{2.21b}$$

$$(-\mathrm{i}n_0 + 3U')\frac{\partial^3 \phi}{\partial x^3} + g\eta''' + U\frac{\partial^4 \phi}{\partial x^4} = 0, \tag{2.21c}$$

from (2.19). These two sets of equations can be combined into equations in η only by using (2.17) to eliminate ϕ. Although there are many (actually infinite) ways to achieve this goal, as we pointed out before, it will be more useful to derive a fourth-order ordinary differential equation with the Class 1 terms in the coefficients the same as the coefficients in (2.3). Bearing this in mind and following a great deal of algebraic manipulation, we finally obtain

$$\begin{aligned} U^4\eta^{\mathrm{iv}} + \eta'''\left[-4\mathrm{i}n_0U^3\right] + \eta''\left[-6n_0^2U^2 + g^2\right] + \eta'\left[4\mathrm{i}n_0^3U\right] \\ +\eta\left[n_0^4 - g^2k_y^2 + \mathrm{i}U'\left\{-6gkk_xU + 2(gk)^{3/2} + 4\frac{g^{3/2}k_x^2}{k^{1/2}}\right\}\right] = 0, \end{aligned} \tag{2.22}$$

in which the Class 1 coefficients are indeed the same as the coefficients of the quartic equation (2.3). Note that the dispersion relation (2.2) and the relation $A = -\mathrm{i}a(g/k)^{1/2}$ can be derived by substitution of (2.6) and (2.7) into the two free-surface boundary conditions (2.18) and (2.19) and by neglect of all the Class 2 terms. Differentiation of these two relations results in relations between k_x' and U' and between a' and A' respectively. The latter leads to cancellation of all the coefficients containing a' and A' in (2.22), while the former has been utilized to eliminate k_x' in favour of U' in (2.22).

Since in deriving (2.22), only a single wave component is under consideration and k_x cannot be eliminated from (2.22) through any further treatment, it is apparent that this equation can truly describe only one individual component (though from the Class 1 terms it seems to have four independent solutions corresponding to the k_{x1}, k_{x2}, k_{x3} and k_{x4} components in figure 1) and is singular at the caustic. Nevertheless, this equation will later be decomposed into a first-order differential equation, which

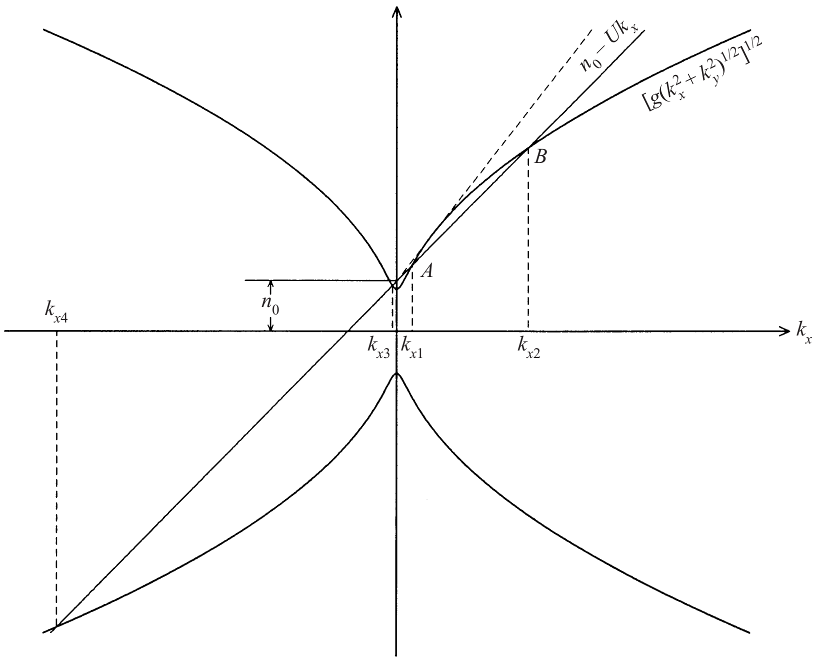

FIGURE 1. Solutions of the dispersion relation (2.3) for given n_0. The dashed line represents the situation occurring at the caustic where the solution points A and B coalesce and therefore $k_{x1} = k_{x2}$.

either for the incident or for the reflected wave is again singular at the caustic, but a combination of them can result in a uniformly valid second-order ordinary differential equation.

3. The equation coupling the incident and reflected waves

The technique for decomposing a higher-order differential equation into a lower-order one in a general asymptotic analysis was given by Turrittin (1952) (also see Wasow 1985). For the special case of decomposing (2.22), refer to Shyu & Phillips (1990). Since each time the procedure can decrease the order of equation only by one, this procedure must be conducted three times. The result is

$$\eta' - \eta[\mathrm{i}k_{x1} + \mathrm{i}R_1] = 0, \tag{3.1}$$

where

$$R_1 = \frac{1}{k_{x1} - k_{x2}}(\hat{P}_1 + \mathrm{i}k_{x1}\hat{Q}_1 + \mathrm{i}k'_{x1}), \tag{3.2}$$

$$\hat{P}_1 = \frac{1}{(k_{x3} - k_{x1})(k_{x3} - k_{x2})}\left\{\frac{-b_1}{(k_{x2} - k_{x4})(k_{x4} - k_{x1})}[k_{x3}k_{x4} - (k_{x1} + k_{x2})(k_{x3} + k_{x4})\right.$$
$$+k_{x1}k_{x2} + (k_{x1}^2 + k_{x2}^2)] + \mathrm{i}\frac{k_{x3} - k_{x2}}{k_{x4} - k_{x1}}(k_{x3} + k_{x4} - 2k_{x1})k_{x2}k'_{x1}$$
$$\left. + \mathrm{i}\frac{k_{x3} - k_{x1}}{k_{x4} - k_{x2}}(k_{x3} + k_{x4} - 2k_{x2})k_{x1}k'_{x2}\right\}, \tag{3.3}$$

$$\hat{Q}_1 = \frac{1}{(k_{x3}-k_{x1})(k_{x3}-k_{x2})}\left\{\frac{\mathrm{i}b_1}{(k_{x2}-k_{x4})(k_{x4}-k_{x1})}(k_{x3}+k_{x4}-k_{x2}-k_{x1}) - \frac{k_{x3}-k_{x2}}{k_{x4}-k_{x1}}\right.$$
$$\left.\times(k_{x3}+k_{x4}-2k_{x1})k'_{x1} - \frac{k_{x3}-k_{x1}}{k_{x4}-k_{x2}}(k_{x3}+k_{x4}-2k_{x2})k'_{x2}\right\}, \quad (3.4)$$

and

$$b_1 = \mathrm{i}U'\left[6\frac{gk_1k_{x1}}{U^3} - 2\frac{(gk_1)^{3/2}}{U^4} - 4\frac{g^{3/2}k_{x1}^2}{U^4k_1^{1/2}}\right]. \quad (3.5)$$

Since the four eigenvalues of the matrix composed of the Class 1 terms in the coefficients of (2.22) are identical with the four roots k_{x1}, k_{x2}, k_{x3} and k_{x4} of (2.3) multiplied by $\mathrm{i} \equiv \sqrt{-1}$, these four wavenumber components enter (3.1) symmetrically.

To obtain (3.1), the parameter k_x in (2.22) has been fixed as the wavenumber component k_{x1} of the incident wave such that (3.1), including its Class 1 and Class 2 terms, can truly describe the incident wave in the regions away from the caustic. The corresponding equation for the reflected wave can directly be obtained from interchange of k_{x1} and k_{x2} in (3.1)–(3.4) and from replacement of k_1 and k_{x1} by k_2 and k_{x2} respectively in (3.5), giving

$$\eta' - \eta[\mathrm{i}k_{x2} + \mathrm{i}R_2] = 0 \quad (3.6)$$

with

$$R_2 = \frac{1}{k_{x2}-k_{x1}}(\hat{P}_2 + \mathrm{i}k_{x2}\hat{Q}_2 + \mathrm{i}k'_{x2}), \quad (3.7)$$

where $\hat{P}_2$ and $\hat{Q}_2$ take the same forms as (3.3) and (3.4) except that b_1 is replaced by

$$b_2 = \mathrm{i}U'\left[6\frac{gk_2k_{x2}}{U^3} - 2\frac{(gk_2)^{3/2}}{U^4} - 4\frac{g^{3/2}k_{x2}^2}{U^4k_2^{1/2}}\right]. \quad (3.8)$$

Both (3.1) and (3.6) are singular at the caustic where $k_{x1} = k_{x2}$ (see figure 1), which is not unexpected as the reflection phenomenon cannot be described by a first-order differential equation. Nevertheless, a combination of them into a second-order equation can couple the incident wave with the reflected wave and in the meantime cancel out the singularities from the equation. Note that during the decomposition we have already obtained a second-order equation before (3.1) was reached, but this equation cannot describe the incident and reflected waves simultaneously, therefore is singular at the caustic.

Intuitively, we may combine (3.1) with (3.6) as

$$\left\{\frac{\partial}{\partial x} - \mathrm{i}[k_{x2}+R_2]\right\}\left\{\frac{\partial}{\partial x} - \mathrm{i}[k_{x1}+R_1]\right\}\eta = 0, \quad (3.9)$$

but it can describe only the k_1-component, because the coefficient k_{x1} in (3.9) is not constant (the differentiation of the Class 2 term R_1 with respect to x is however negligible within the present approximation). An expansion of (3.9) yields

$$\eta'' - \left[\mathrm{i}(k_{x1}+k_{x2}) + \mathrm{i}(R_1+R_2)\right]\eta' - \left[k_{x1}k_{x2} + (k_{x2}R_1 + k_{x1}R_2) + \mathrm{i}k'_{x1}\right]\eta = 0, \quad (3.10)$$

which is obviously not symmetric with respect to k_{x1} and k_{x2}. To solve this problem, we add, from (3.1) and neglecting the products of two Class 2 terms,

$$\frac{k'_{x1}-k'_{x2}}{k_{x2}-k_{x1}}\eta' - \mathrm{i}k_{x1}\frac{k'_{x1}-k'_{x2}}{k_{x2}-k_{x1}}\eta = 0 \quad (3.11)$$

to (3.10), resulting in

$$\eta'' + [-\mathrm{i}(k_{x1} + k_{x2}) + Q]\eta' + [-k_{x1}k_{x2} + P]\eta = 0, \tag{3.12}$$

where

$$\left.\begin{aligned} P &= -(k_{x2}R_1 + k_{x1}R_2) - \mathrm{i}\frac{k_{x2}k'_{x1} - k_{x1}k'_{x2}}{k_{x2} - k_{x1}}, \\ Q &= -\mathrm{i}(R_1 + R_2) + \frac{k'_{x1} - k'_{x2}}{k_{x2} - k_{x1}}. \end{aligned}\right\} \tag{3.13}$$

Since (3.10) and (3.11) can both be fulfilled by the k_1-component and on the other hand (3.12) together with (3.13) is symmetric with respect to k_{x1} and k_{x2}, it is obvious that the two independent solutions of (3.12) will correspond to the k_1- and k_2-components. Furthermore, in the following section we shall prove that all singularities can be cancelled out from (3.12) so that as a multiple-scale asymptotic approximation, this equation can be valid virtually everywhere including the caustic. Note that in view of (3.2)–(3.5), (3.7), (3.8) and (3.13), the parameters P and Q in (3.12) indeed represent the Class 2 coefficients.

4. Proof of regularity

The sufficient condition for (3.12) being regular at the caustic is that the coefficients in (3.12) are all regular at this point. Since k_{x1} and k_{x2} are a pair of solutions of the quartic equation (2.3) which become identical with each other at the simple turning point (the following argument will not hold for the triple turning point suggested and investigated by Trulsen & Mei 1993), they can be divided into two parts:

$$k_{x1} = M - N, \qquad k_{x2} = M + N, \tag{4.1}$$

where N and $-N$ are two branches of a double-valued function, say $\psi^{1/2}$, which equals zero at the caustic, and M and ψ are both regular at this point. From the above,

$$N^2 = \psi, \qquad NN' = \tfrac{1}{2}\psi', \tag{4.2}$$

so that N^2, NN', N^4, N^3N', etc. are all regular at the caustic. Therefore we shall in the following prove that when (4.1) are substituted in (3.12) and (3.13), only this kind of term and the terms without N can survive cancellation.

First, from (4.1),

$$k_{x1} + k_{x2} = 2M, \qquad k_{x1}k_{x2} = M^2 - N^2.$$

Therefore the Class 1 terms in (3.12) are obviously regular. Next, from (3.13), (3.2) and (3.7), we have

$$\left.\begin{aligned} P &= \frac{-1}{k_{x1} - k_{x2}}\left[(k_{x2}\hat{P}_1 - k_{x1}\hat{P}_2) + \mathrm{i}k_{x1}k_{x2}(\hat{Q}_1 - \hat{Q}_2)\right], \\ Q &= \frac{-1}{k_{x1} - k_{x2}}\left[\mathrm{i}(\hat{P}_1 - \hat{P}_2) - (k_{x1}\hat{Q}_1 - k_{x2}\hat{Q}_2)\right]. \end{aligned}\right\} \tag{4.3}$$

Recall that the only difference between $\hat{P}_1$ and $\hat{P}_2$ or between $\hat{Q}_1$ and $\hat{Q}_2$ is that the former involves b_1 while the latter involves b_2 in (3.3) or (3.4). Thus we have

$$\begin{aligned} \hat{P}_1 - \hat{P}_2 = \frac{1}{L}\big[&-k_{x3}k_{x4} + (k_{x1} + k_{x2})(k_{x3} + k_{x4}) \\ &-k_{x1}k_{x2} - (k_{x1}^2 + k_{x2}^2)\big](b_1 - b_2), \end{aligned} \tag{4.4a}$$

$$\hat{Q}_1 - \hat{Q}_2 = \frac{\mathrm{i}}{L}(k_{x3} + k_{x4} - k_{x2} - k_{x1})(b_1 - b_2), \tag{4.4b}$$

$$\begin{aligned} k_{x2}\hat{P}_1 - k_{x1}\hat{P}_2 = \frac{1}{L}\{ & [-k_{x3}k_{x4} + (k_{x1} + k_{x2})(k_{x3} + k_{x4}) - k_{x1}k_{x2} - (k_{x1}^2 + k_{x2}^2)] \\ & \times (k_{x2}b_1 - k_{x1}b_2) + \mathrm{i}(k_{x1} - k_{x2}) \\ & \times [(k_{x3} + k_{x4} - 2k_{x1})(k_{x3} - k_{x2})(k_{x4} - k_{x2})k_{x2}k'_{x1} \\ & + (k_{x3} + k_{x4} - 2k_{x2})(k_{x3} - k_{x1})(k_{x4} - k_{x1})k_{x1}k'_{x2}]\}, \end{aligned} \tag{4.4c}$$

and

$$\begin{aligned} k_{x1}\hat{Q}_1 - k_{x2}\hat{Q}_2 = \frac{1}{L}\{ & \mathrm{i}(k_{x3} + k_{x4} - k_{x2} - k_{x1})(k_{x1}b_1 - k_{x2}b_2) + (k_{x1} - k_{x2}) \\ & \times [(k_{x3} + k_{x4} - 2k_{x1})(k_{x3} - k_{x2})(k_{x4} - k_{x2})k'_{x1} \\ & + (k_{x3} + k_{x4} - 2k_{x2})(k_{x3} - k_{x1})(k_{x4} - k_{x1})k'_{x2}]\}, \end{aligned} \tag{4.4d}$$

where

$$L = (k_{x3} - k_{x1})(k_{x3} - k_{x2})(k_{x2} - k_{x4})(k_{x4} - k_{x1}). \tag{4.4e}$$

From (3.5) and (3.8) and by using (2.2), we also have

$$\begin{aligned} b_1 - b_2 = \mathrm{i}(k_{x1} - k_{x2})\frac{U'}{U^2}\Bigg\{ & \frac{12}{U}n_0^2 + 8UT - 18n_0(k_{x1} + k_{x2}) - \frac{1}{k_1^2k_2^2} \\ & \times \Bigg[4k_y^2\frac{n_0^3}{U^2}(k_{x1} + k_{x2}) + 12n_0k_y^2S \\ & - 12k_y^2\frac{n_0^2}{U}T - 4Uk_y^2(k_{x1}^4 + k_{x2}^4) - 4Uk_y^2k_{x1}k_{x2}T \\ & + 12n_0k_{x1}^2k_{x2}^2\left(k_{x1} + k_{x2} - \frac{n_0}{U}\right) - 4Uk_{x1}^2k_{x2}^2T\Bigg]\Bigg\}, \end{aligned} \tag{4.5a}$$

$$\begin{aligned} k_{x2}b_1 - k_{x1}b_2 = \mathrm{i}(k_{x1} - k_{x2})\frac{U'}{U^2}\Bigg\{ & 8Uk_{x1}k_{x2}(k_{x1} + k_{x2}) - 18n_0k_{x1}k_{x2} + 2\frac{n_0^3}{U^2} - \frac{1}{k_1^2k_2^2} \\ & \times \Bigg[4k_y^2\frac{n_0^3}{U^2}k_{x1}k_{x2} + 12n_0k_y^2k_{x1}k_{x2}T - 12k_y^2\frac{n_0^2}{U}k_{x1}k_{x2}(k_{x1} + k_{x2}) \\ & - 4Uk_y^2k_{x1}k_{x2}S - 4\frac{n_0^3}{U^2}k_{x1}^2k_{x2}^2 + 12n_0k_{x1}^3k_{x2}^3 - 4Uk_{x1}^3k_{x2}^3(k_{x1} + k_{x2})\Bigg]\Bigg\}, \end{aligned} \tag{4.5b}$$

and

$$\begin{aligned} k_{x1}b_1 - k_{x2}b_2 = \mathrm{i}(k_{x1} - k_{x2})\frac{U'}{U^2}\Bigg\{ & 12\frac{n_0^2}{U}(k_{x1} + k_{x2}) + 8US - 18n_0T - 2\frac{n_0^3}{U^2} - \frac{1}{k_1^2k_2^2} \\ & \times \Bigg[4k_y^2\frac{n_0^3}{U^2}T + 12n_0k_y^2(k_{x1}^4 + k_{x2}^4) + 12n_0k_y^2k_{x1}k_{x2}T \\ & - 12k_y^2\frac{n_0^2}{U}S + 4\frac{n_0^3}{U^2}k_{x1}^2k_{x2}^2 - 4Uk_y^2(k_{x1}^3 + k_{x2}^3)T \\ & + 12n_0k_{x1}^2k_{x2}^2T - 12\frac{n_0^2}{U}k_{x1}^2k_{x2}^2(k_{x1} + k_{x2}) - 4Uk_{x1}^2k_{x2}^2S\Bigg]\Bigg\}, \end{aligned} \tag{4.5c}$$

where

$$S = (k_{x1} + k_{x2})(k_{x1}^2 + k_{x2}^2), \qquad T = k_{x1}^2 + k_{x2}^2 + k_{x1}k_{x2}. \tag{4.5d}$$

Therefore, from (4.4) and (4.5) it is clear that the denominator $k_{x1} - k_{x2}$ in (4.3) can be eliminated from both P and Q, after which they become symmetric about k_{x1} and k_{x2} so that when (4.1) is employed, all terms containing odd power of N (including N') will be cancelled out, ensuring that (3.12) is regular at the turning point. Hence one may expect that (3.12) is uniformly valid near and away from the turning point.

The values of P and Q at the caustic can be calculated exactly by using (4.3), (4.4) and (4.5), but in order to do that, it is necessary to substitute (4.1) into (4.4*c*) and (4.4*d*) to eliminate k'_{x1} and k'_{x2} (which become infinite at the caustic) in favour of M' and NN'. Both M' and NN' are regular at the caustic as mentioned before, and since at this point,

$$U + C_{gx1} = U + C_{gx2} = 0,$$

it is not difficult to obtain from the dispersion relation (2.2)

$$NN' = \frac{n_0 - U_0 M_0}{n_0 + 2U_0 M_0} \frac{M_0^2}{U_0} U', \tag{4.6}$$

$$M' = \left[\frac{1}{3} \left(\frac{n_0}{U_0} - 8M_0 \right) \frac{M_0}{n_0 + 2U_0 M_0} + \frac{2}{3} \frac{M_0}{U_0} \frac{n_0^2 - U_0^2 M_0^2}{(n_0 + 2U_0 M_0)^2} \right] U', \tag{4.7}$$

at this point, where U_0 and M_0 are the values of U and M at the same point. Hence the calculations of singularities can now be avoided completely.

Finally, we note that from (2.17*a*), (2.18), (2.19) and the relation

$$\left.\frac{\partial \phi}{\partial x}\right|_{z=0} = \left(\mathrm{i}k_x + \frac{A'}{A} \right) \phi$$

resulting from (2.7), one may directly obtain two first-order equations for the incident and reflected waves, which are much simpler than (3.1) and (3.6). These two equations can also be combined into a second-order equation and proven regular at the caustic. However, in this second-order equation, the Class 2 coefficients corresponding to P and Q in (3.12) cannot be calculated accurately at the caustic, because after all substitutions and reductions, they still contain two terms which are both singular at the caustic, though their singularities can balance each other. Another disadvantage of this simpler equation is that when $k_y = 0$, the expressions for the Class 2 terms in this equation cannot be reduced to those in (6.3) of Shyu & Phillips (1990), but (3.13) can be reduced to (6.4) in Shyu & Phillips (1990).

5. Solutions of reflection phenomenon

The equation (3.12) in terms of the parameters k_{x1}, k_{x2}, P and Q takes the same form as those derived by Shyu & Phillips (1990) so that the uniformly valid asymptotic solution of (3.12) can similarly be derived using the treatment suggested by the results of Smith (1975).

Following the precedent of Shyu & Phillips (1990), we first eliminate the first-derivative term from (3.12) by a change of the dependent variable η, such that

$$\eta = v(x) \exp\left\{ -\frac{1}{2} \int_0^x [-\mathrm{i}(k_{x1} + k_{x2}) + Q]\,\mathrm{d}x \right\} \exp \mathrm{i}(k_y y - n_0 t), \tag{5.1}$$

where $v(x)$ is the new dependent variable. Next, substituting (5.1) into (3.12) and neglecting the higher-order terms involving Q' and Q^2, we obtain

$$v'' + v(H + G) = 0, \tag{5.2}$$

where

$$H = \tfrac{1}{4}(k_{x2} - k_{x1})^2, \tag{5.3}$$

$$G = P + \frac{\mathrm{i}}{2}(k_{x1} + k_{x2})Q + \frac{\mathrm{i}}{2}(k'_{x1} + k'_{x2}), \tag{5.4}$$

so that H represents the Class 1 term and G the Class 2 term. Equation (5.2) is still regular at the caustic, and from Smith's (1975) results, we expect that

$$v(x) \approx A_0 \mathrm{Ai}\,(-r) - C_0 \mathrm{Ai}'\,(-r), \tag{5.5}$$

where $\mathrm{Ai}'\,(-r) = \{\mathrm{dAi}\,(x)/\mathrm{d}x\}_{x=-r}$ and

$$\tfrac{2}{3}r^{3/2} = -\int_0^x H^{1/2}\,\mathrm{d}x, \tag{5.6a}$$

$$A_0 = \left(\frac{r}{H}\right)^{1/4} \cos\left(-\int_0^x \tfrac{1}{2}G/H^{1/2}\,\mathrm{d}x\right), \tag{5.6b}$$

$$C_0 = r^{-1/4}H^{-1/4} \sin\left(-\int_0^x \tfrac{1}{2}G/H^{1/2}\,\mathrm{d}x\right). \tag{5.6c}$$

For the sake of definiteness, we have taken $x = 0$ to be the caustic and assumed that $H > 0$ for $x < 0$, corresponding to a situation in which the reflected wave is shorter and its group velocity component in the x-direction smaller than the incident wave (see figure 1 and recall that $C_{gx} = \partial\sigma/\partial k_x$).

The fitness of (5.5) and (5.6) can easily be verified by substituting them into (5.2), which results in

$$\frac{\mathrm{d}^2 v}{\mathrm{d}x^2} + v(H + G) = \frac{\mathrm{d}^2 A_0}{\mathrm{d}x^2}\mathrm{Ai}\,(-r) - \frac{\mathrm{d}^2 C_0}{\mathrm{d}x^2}\mathrm{Ai}'\,(-r) \tag{5.7}$$

as $\mathrm{Ai}''\,(-r)$ is eliminated in favour of $-r\mathrm{Ai}\,(-r)$. Since the coefficients A_0 and C_0 in (5.5) have been separated from the rapidly varying parts of the solution, the terms on the right-hand side of (5.7) are again negligible so that the differences between (5.2) and (5.7) are insignificant. Furthermore, if A_0 and C_0 are regular and therefore remain slowly varying at the caustic, the solution (5.5) (and (5.1)) is also regular here and will satisfy the equation (5.2) everywhere, including the caustic, within the present approximation. Therefore we shall demonstrate the regularity of A_0 and C_0 at the caustic in the following way.

In the vicinity of the caustic, from (4.1), (4.2) and the Taylor's theorem, we have

$$H = \tfrac{1}{4}(k_{x2} - k_{x1})^2 = N^2 = \psi_1 x + \psi_2 x^2 + \cdots,$$

where $\psi_1 = \mathrm{d}\psi/\mathrm{d}x|_{x=0}$ and $2\psi_2 = \mathrm{d}^2\psi/\mathrm{d}x^2|_{x=0}$. Thus

$$\left.\begin{aligned} -\int_0^x H^{1/2}\,\mathrm{d}x &= (-\psi_1)^{1/2}(-x)^{3/2}\left[\frac{2}{3} + \frac{1}{5}\frac{\psi_2}{\psi_1}x + \cdots\right], \\ -\int_0^x \frac{1}{2}G/H^{1/2}\,\mathrm{d}x &= G_0(-\psi_1)^{-1/2}(-x)^{1/2}\left[1 + \left(\frac{1}{3}\frac{G_1}{G_0} - \frac{1}{6}\frac{\psi_2}{\psi_1}\right)x + \cdots\right], \end{aligned}\right\} \tag{5.8}$$

where $G = G_0 + G_1 x + \cdots$. Substituting (5.8) in (5.6), we obtain

$$\left.\begin{aligned} r &= (-\psi_1)^{1/3}(-x)\left[1 + \frac{1}{5}\frac{\psi_2}{\psi_1}x + \cdots\right], \\ A_0 &= (-\psi_1)^{-1/6}\left[1 - \left(\frac{1}{5}\frac{\psi_2}{\psi_1} + \frac{1}{2}\frac{G_0^2}{\psi_1}\right)x + \cdots\right], \\ C_0 &= G_0(-\psi_1)^{-5/6}\left[1 - \left(\frac{7}{15}\frac{\psi_2}{\psi_1} - \frac{1}{3}\frac{G_1}{G_0}\right)x + \cdots\right], \end{aligned}\right\} \tag{5.9}$$

in this region. Since the expressions in (5.9) represent the Taylor-series expansions about $x = 0$ and their radii of convergence can be expected to be very large for a slowly varying current field, A_0, C_0 and r are indeed regular at the caustic. Therefore (5.1) together with (5.5) and (5.6) represents a uniformly valid asymptotic solution.

At points away from the caustic, $\mathrm{Ai}\,(-r)$ and $\mathrm{Ai}'\,(-r)$ can be replaced by their asymptotic approximations, which for r large and positive are

$$\mathrm{Ai}\,(-r) \approx \pi^{-1/2} r^{-1/4} \sin\left(\tfrac{2}{3} r^{3/2} + \tfrac{1}{4}\pi\right), \tag{5.10}$$

$$\mathrm{Ai}'\,(-r) \approx -\pi^{-1/2} r^{1/4} \cos\left(\tfrac{2}{3} r^{3/2} + \tfrac{1}{4}\pi\right). \tag{5.11}$$

Thus from (5.1), (5.5) and (5.6), we have

$$\begin{aligned} \eta \approx{}& H^{-1/4}\exp\left[\int_0^x \tfrac{1}{2}(-Q - \mathrm{i}G/H^{1/2})\,\mathrm{d}x\right]\exp\mathrm{i}\left[\int_0^x k_{x1}\,\mathrm{d}x + k_y y - n_0 t - \tfrac{1}{4}\pi\right] \\ &+ H^{-1/4}\exp\left[\int_0^x \tfrac{1}{2}(-Q + \mathrm{i}G/H^{1/2})\,\mathrm{d}x\right]\exp\mathrm{i}\left[\int_0^x k_{x2}\,\mathrm{d}x + k_y y - n_0 t + \tfrac{1}{4}\pi\right] \end{aligned} \tag{5.12}$$

for $x \ll 0$. This solution represents the WKBJ approximation; it obviously fails at the caustic where $H = 0$, but can nevertheless indicate the existence of the incident and reflected waves, as well as show their relative amplitudes and phases (an irrelevant constant common factor was neglected from (5.12)). Consequently, we have the local amplitudes

$$a = \begin{cases} H^{-1/4}\exp\left[\int_0^x \tfrac{1}{2}(-Q - \mathrm{i}G/H^{1/2})\,\mathrm{d}x\right] & (k_1 \text{ component}) \\ H^{-1/4}\exp\left[\int_0^x \tfrac{1}{2}(-Q + \mathrm{i}G/H^{1/2})\,\mathrm{d}x\right] & (k_2 \text{ component}) \end{cases} \tag{5.13}$$

(notice that G is pure imaginary while H and Q are real), which have been proved to satisfy the action conservation principle at and away from the caustic.

6. Extensions to general cases

A difference between Smith's (1975) theory and the present theory is that in the latter, the expressions for the amplitudes of the incident and reflected waves take an explicit form while in the former, the variations of these quantities were demonstrated to fulfil the action conservation principle everywhere, including the caustic. The present expressions, especially those in (5.13), if also valid in a general situation, will later prove of great use in the improvement of an error magnification phenomenon occurring in the estimates of the amplitude of the reflected wave in terms of that of the incident wave in the vicinity of the caustic during a numerical computation, which

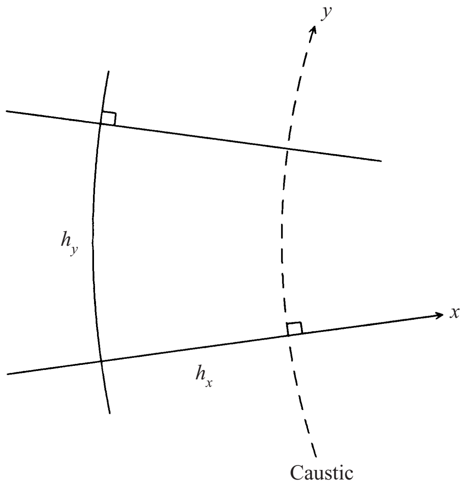

FIGURE 2. Definition sketch.

are required for the ray solution to be continued after reflection at the caustic. To achieve this goal, we shall in this section demonstrate that even when the water is of intermediate depth and the underlying larger-scale irrotational flow is multidirectional and unsteady, the solutions of the wave field in the vicinity of the caustic still take the same forms as those derived in Shyu & Phillips (1990) and in the preceding section.

When the larger-scale flows are not unidirectional, the caustics are unlikely to be straight. Thus it is necessary to derive the solutions in a set of orthogonal curvilinear coordinates in which the x-axis is perpendicular to the caustic. Therefore we define all the lines $x =$ constant to be parallel curves and $x = 0$ corresponds to the caustic (see figure 2), so that the scale factor h_x in the x-direction is independent of the position. On the other hand, if at the caustic we set the scale factor in the y-direction $h_y = 1$, the variation of h_y in the x-direction has the simple relation

$$h_y = 1 - \frac{x}{R(y,t)} \tag{6.1}$$

where R is the radius of curvature of the caustic which is large compared with the wavelength if the underlying current is slowly varying. This coordinate system will certainly produce singularities of the differential equations at certain positions far away from the caustic, but since it is the present purpose to derive the solutions in the vicinity of the caustic, these singularities can be avoided in the present analysis.

In this curvilinear coordinate system, the WKBJ solution of each wave component can still be written as

$$\eta = a(x,y,t)\exp[\mathrm{i}\chi(x,y,t)], \tag{6.2}$$

although the forms of the functions $a(x,y,t)$ and $\chi(x,y,t)$ in (6.2) are different from those in a rectangular coordinate system. From (6.2), the x- and y-components of the wavenumber and the observed frequency are

$$k_x = \frac{\partial\chi}{\partial x}, \qquad k_y = \frac{1}{h_y}\frac{\partial\chi}{\partial y}, \qquad n = -\frac{\partial\chi}{\partial t}, \tag{6.3}$$

respectively. In (6.2) and (6.3), the dependence of a, k_x, k_y and n on x, y and t is expected to be slow except that in the vicinity of the caustic the variations of a and k_x

with x will be rapid owing to the singularities at the caustic. Notice that the variations of h_y with x, y, t are also slow in view of (6.1).

From (6.2) and (6.3), equations (3.1) and (3.6) immediately follow with

$$R_1 = -\mathrm{i}\frac{a_1'}{a_1}, \qquad R_2 = -\mathrm{i}\frac{a_2'}{a_2}. \tag{6.4}$$

The values of a_1'/a_1 and a_2'/a_2 cannot be determined without consideration of the Laplace equation and the kinematical and dynamical boundary conditions, which even in the vicinity of the caustic can result in the action conservation equation as demonstrated by Smith (1975) in exactly the same circumstance, who also derived the dispersion relation in this region which is again identical with that far from the caustic. Notice that although the WKBJ solution becomes invalid in the immediate vicinity of the caustic, the solution values of a_1, a_2, k_1 and k_2 in this region determined from the action conservation equation and the dispersion relation are still meaningful, because a combination of these parameters can represent the quantities in the uniformly valid solution (see (1.1) and (1.2)).

Next, following the same procedure as in § 3, we again obtain (3.12) together with (3.13). Thus if we choose

$$\eta = v(x, y, t)\exp\left\{\frac{\mathrm{i}}{2}(\chi_1 + \chi_2) - \int_0^x \frac{Q}{2}\,\mathrm{d}x\right\}, \tag{6.5}$$

which equivalent to (5.1) for a straight caustic, we can similarly achieve

$$v(x, y, t) = A_0\mathrm{Ai}\,(-r) - C_0\mathrm{Ai}'\,(-r) \tag{6.6}$$

with

$$\tfrac{2}{3}r^{3/2} = -\int_0^x H^{1/2}\,\mathrm{d}x, \tag{6.7}$$

$$A_0 = \left(\frac{r}{H}\right)^{1/4}\cos\left(-\int_0^x \tfrac{1}{2}G/H^{1/2}\,\mathrm{d}x\right), \quad C_0 = r^{-1/4}H^{-1/4}\sin\left(-\int_0^x \tfrac{1}{2}G/H^{1/2}\,\mathrm{d}x\right), \tag{6.8}$$

in which

$$H = \tfrac{1}{4}(k_{x2} - k_{x1})^2, \tag{6.9}$$

$$G = P + \frac{\mathrm{i}}{2}(k_{x1} + k_{x2})Q + \frac{\mathrm{i}}{2}(k_{x1}' + k_{x2}'). \tag{6.10}$$

The new variable r now depends on x, y and t, but its variations with respect to y and t will be slow.

The adequacy of (6.5)–(6.10) as a uniformly valid solution for the case of a curved and/or moving caustic in a deep or intermediate-depth region, depends on whether the singularities at the caustic can be cancelled out from $\chi_1 + \chi_2$, Q, G, etc., otherwise the above solution will become singular here and the coefficients A_0 and C_0 are no longer slowly varying in the vicinity of the caustic, which will decline the use of the approximation implied by (5.7). Therefore it is required in the following to demonstrate the regularity of (6.5)–(6.10) at the caustic.

Even for a curved moving caustic in an intermediate-depth region, from the dispersion relation and the fact that $U_x + C_{gx} = 0$ at the caustic, one can always prove that k_{x1} and k_{x2} represent two branches of a double-valued function with the branch point at the caustic $x=0$. Therefore the phase function of the incident wave can be written as

$$\chi_1 = [d_0 + d_1 x + d_2 x^2 + \cdots] + \tfrac{2}{3}\left[(-\psi_1)^{1/3}(-x) + O(x^2)\right]^{3/2} \tag{6.11}$$

(also see (9), Smith 1975), where the coefficients of the Taylor series expansions about $x=0$ in the two square brackets are functions of y and t, which except d_0 are slowly varying according to the discussion following (6.3). On substitution χ_1 into (6.3) we have

$$\left.\begin{aligned} k_{x1} &= [d_1 + 2d_2 x + O(x^2)] - [\psi_1 x + O(x^2)]^{1/2},\\ h_y k_{y1} &= \left[\frac{\partial d_0}{\partial y} + \frac{\partial d_1}{\partial y}x + O(x^2)\right] - \frac{1}{3}\frac{\partial \psi_1}{\partial y}\left[(-\psi_1)^{-1}(-x)^3 + O(x^4)\right]^{1/2}. \end{aligned}\right\} \tag{6.12}$$

The other branches of (6.11) and (6.12) then provide respectively the phase and wave-number components of the reflected wave:

$$\chi_2 = [d_0 + d_1 x + d_2 x^2 + \cdots] - \tfrac{2}{3}\left[(-\psi_1)^{1/3}(-x) + O(x^2)\right]^{3/2}, \tag{6.13}$$

$$\left.\begin{aligned} k_{x2} &= [d_1 + 2d_2 x + O(x^2)] + [\psi_1 x + O(x^2)]^{1/2},\\ h_y k_{y2} &= \left[\frac{\partial d_0}{\partial y} + \frac{\partial d_1}{\partial y}x + O(x^2)\right] + \frac{1}{3}\frac{\partial \psi_1}{\partial y}\left[(-\psi_1)^{-1}(-x)^3 + O(x^4)\right]^{1/2}. \end{aligned}\right\} \tag{6.14}$$

The above phase functions not only lead to the right forms of k_{x1} and k_{x2}, but also ensure that $\nabla \times \boldsymbol{k} = 0$ for both waves. However, the values of the series coefficients d_1, d_2, ψ_1, etc. can be determined only from the dispersion relation. We notice in passing that for a curved caustic, even though k_{y1} is not equal to k_{y2} when $x \neq 0$, their difference is much smaller than that between k_{x1} and k_{x2} and is proportional approximately to $(-x)^{3/2}$ (also with a smaller coefficient $(\frac{2}{3})(-\psi_1)^{-1/2}\partial\psi_1/\partial y$) when the caustic is approached. A similar situation also occurs to the observed frequencies n_1 and n_2 of the incident and reflected waves for a moving caustic. These situations can benefit the numerical computations of the reflected wave significantly as will be seen in the next section. Also we emphasize that neglect of the higher powers of x in the Taylor series expansion of a slowly varying parameter is equivalent to neglect of its higher-order derivatives with respect to x, because the series coefficients are closely related to the derivatives of the same order.

From (6.11) and (6.13) it is immediately clear that $\chi_1 + \chi_2$ in (6.5) is regular at the caustic. On the other hand, from (6.12) and (6.14), we have in the vicinity of the caustic

$$H = \tfrac{1}{4}(k_{x2} - k_{x1})^2 = \psi_1 x + O(x^2). \tag{6.15}$$

Consequently

$$-\int_0^x H^{1/2}\,\mathrm{d}x = \tfrac{2}{3}(-\psi_1)^{1/2}(-x)^{3/2}[1 + O(x)] \tag{6.16}$$

and

$$-\int_0^x \tfrac{1}{2}G/H^{1/2}\,\mathrm{d}x = G_0(-\psi_1)^{-1/2}(-x)^{1/2}[1 + O(x)] \tag{6.17}$$

if G is regular at the caustic and $G_0 \equiv G(x=0)$. Substitution of (6.16) into (6.7) results in

$$r = (-\psi_1)^{1/3}(-x)[1 + O(x)]. \tag{6.18}$$

Again the radius of convergence of the power series in the square brackets in (6.18) can be expected to be large compared with the wavelength as long as the underlying current is slowly varying. Therefore (6.18) indicates that r is regular at the caustic. Furthermore, on substituting (6.15), (6.17) and (6.18) into (6.8), we have

$$A_0 = (-\psi_1)^{-1/6}[1 + O(x)], \quad C_0 = G_0(-\psi_1)^{-5/6}[1 + O(x)], \tag{6.19}$$

in the vicinity of the caustic, so that A_0 and C_0 are also regular (and therefore slowly varying) at the caustic. All of these results enable us to conclude that the singularities at the caustic have been cancelled out from the solution (6.5)–(6.10) provided that G and Q are also regular here, which will be demonstrated as follows.

Since the parameters G and Q also appear in the WKBJ solution, their regularity can be proved through a consideration of the action conservation equation, the fulfillment of which by the WKBJ solution even in the vicinity of the caustic was demonstrated by Smith (1975). Thus, substituting (5.10) and (5.11) into (6.6), using (6.7) and (6.9), and also taking (6.3) into consideration, we obtain the WKBJ solution

$$\eta = C(y,t)H^{-1/4}\exp\left[\int_0^x \tfrac{1}{2}(-Q - \mathrm{i}G/H^{1/2})\,\mathrm{d}x\right]\exp\mathrm{i}\left(\chi_1 - \tfrac{1}{4}\pi\right)$$
$$+C(y,t)H^{-1/4}\exp\left[\int_0^x \tfrac{1}{2}(-Q + \mathrm{i}G/H^{1/2})\,\mathrm{d}x\right]\exp\mathrm{i}\left(\chi_2 + \tfrac{1}{4}\pi\right), \tag{6.20}$$

where the common factor $C(y,t)$ is independent of x. From (6.20), the local amplitudes of the incident and reflected waves are

$$\left.\begin{aligned} a_1 &= CH^{-1/4}\exp\left[\int_0^x \tfrac{1}{2}(-Q - \mathrm{i}G/H^{1/2})\,\mathrm{d}x\right], \\ a_2 &= CH^{-1/4}\exp\left[\int_0^x \tfrac{1}{2}(-Q + \mathrm{i}G/H^{1/2})\,\mathrm{d}x\right]. \end{aligned}\right\} \tag{6.21}$$

Therefore substitution of (6.15) for H and differentiation yield

$$\frac{a_1'}{a_1} = \tfrac{1}{2}(-Q - \mathrm{i}G/H^{1/2}) - \frac{1}{2}\frac{k_{x2}' - k_{x1}'}{k_{x2} - k_{x1}}, \tag{6.22a}$$

$$\frac{a_2'}{a_2} = \tfrac{1}{2}(-Q + \mathrm{i}G/H^{1/2}) - \frac{1}{2}\frac{k_{x2}' - k_{x1}'}{k_{x2} - k_{x1}}. \tag{6.22b}$$

The above expressions for a_1'/a_1 and a_2'/a_2 are identical with those in (6.4) if the expression (3.13) and the definition (6.10) for G are substituted into (6.4) for R_1 and R_2. This and the fact that (6.20) represents a rigorous asymptotic approximation of the solution (6.5)–(6.10) have put even more confidence in the assumption that if the singularities at the caustic are completely cancelled out from (3.12), this equation and the solution (6.5)–(6.10) will remain valid uniformly in a region containing the caustic.

The variations of a_1 and a_2 have been proved by Smith (1975) to satisfy the action conservation equation in the vicinity of the caustic. Therefore, the regularity of the parameters Q, G in (6.22a,b) at the caustic can be demonstrated through a consideration of the action conservation equation. First, from (6.12) and (6.14) it immediately follows that

$$\frac{1}{2}\frac{k_{x2}' - k_{x1}'}{k_{x2} - k_{x1}} = \frac{1}{4x}[1 + O(x)] \tag{6.23}$$

near the caustic. Next, from the action conservation equation in the curvilinear coordinates

$$\frac{\partial}{\partial t}\left(\frac{E_1}{\sigma_1}\right)+\frac{\partial}{\partial x}\left[(U_x+C_{gx1})\frac{E_1}{\sigma_1}\right]+\frac{1}{h_y}\frac{\partial h_y}{\partial x}\left[(U_x+C_{gx1})\frac{E_1}{\sigma_1}\right]$$
$$+\frac{1}{h_y}\frac{\partial}{\partial y}\left[(U_y+C_{gy1})\frac{E_1}{\sigma_1}\right]=0, \quad (6.24)$$

in which the wave action density of the incident wave

$$\frac{E_1}{\sigma_1}=\tfrac{1}{2}\rho g\frac{a_1^2}{\sigma_1},$$

where E_1 represents its energy density and ρ the density of water. Therefore, substitution and expansion yield

$$\frac{a_1'}{a_1}=-\frac{\sigma_1}{2(U_x+C_{gx1})}\frac{\partial}{\partial x}\left(\frac{U_x+C_{gx1}}{\sigma_1}\right)-\frac{\sigma_1}{2a_1^2(U_x+C_{gx1})}\frac{\partial}{\partial t}\left(\frac{a_1^2}{\sigma_1}\right)$$
$$-\frac{1}{1-x/R}\frac{\sigma_1}{2a_1^2(U_x+C_{gx1})}\frac{\partial}{\partial y}\left[(U_y+C_{gy1})\frac{a_1^2}{\sigma_1}\right]+\frac{1}{2R}\frac{1}{1-x/R} \quad (6.25)$$

by virtue of (6.1).

The relation between σ_1 and k_1 differs according to whether the water is deep or of moderate depth, but in any case, by using (6.12) and the dispersion relation, one can always obtain the form of the expansion

$$\frac{U_x+C_{gx1}}{\sigma_1}=\sqrt{\psi_1 x}[\alpha_0+O(x)]+[e_1x+O(x^2)] \quad (6.26)$$

in the vicinity of the caustic, where α_0 and e_1 are the leading coefficients of the two Taylor series in the square brackets. The absence of e_0 from the second series is simply due to the fact that $U_x+C_{gx1}=0$ at the caustic. Thus from (6.26), the first term on the right-hand side of (6.25)

$$-\frac{\sigma_1}{2(U_x+C_{gx1})}\frac{\partial}{\partial x}\left(\frac{U_x+C_{gx1}}{\sigma_1}\right)=-\frac{1}{4x}[1+O(x)]+\frac{1}{\sqrt{\psi_1 x}}[\beta_0+O(x)] \quad (6.27)$$

near the caustic. Since in the vicinity of the caustic, variations of wave properties perpendicular to the caustic are large compared to variations along the caustic or with time, (6.27) represents the major contribution to a_1'/a_1 in (6.25) in this region. Therefore, from a comparison between (6.27) and (6.23) it is immediately clear that the term $H^{-1/4}$ in a_1 in the present solution (6.21), which leads to the last terms in (6.22*a*, *b*) and therefore (6.23), is indeed consistent with the prediction by the action conservation principle as far as their first approximations are concerned. However, the values of G and Q cannot be obtained without further evaluation of the second and third terms on the right-hand side of (6.25).

Since the first approximation $a_1\approx CH^{-1/4}$ has been justified, from (6.15) we have

$$a_1^2\approx\frac{C^2}{\sqrt{\psi_1 x}} \quad (6.28)$$

near the caustic. Also, from the dispersion relation, it is not difficult to see that the series expansions of σ_1 and U_y+C_{gy1} will possess the same form as that of k_{x1} in (6.12). Thus, using these series and (6.28) as well as (6.26), and recalling that C and

ψ_1 are slow functions of y and t, we obtain

$$-\frac{\sigma_1}{2a_1^2(U_x+C_{gx1})}\frac{\partial}{\partial t}\left(\frac{a_1^2}{\sigma_1}\right) \approx \frac{\xi_0}{\sqrt{\psi_1 x}}, \tag{6.29}$$

$$-\frac{1}{1-x/R}\frac{\sigma_1}{2a_1^2(U_x+C_{gx1})}\frac{\partial}{\partial y}\left[(U_y+C_{gy1})\frac{a_1^2}{\sigma_1}\right] \approx \frac{\zeta_0}{\sqrt{\psi_1 x}}, \tag{6.30}$$

in which the Taylor expansion

$$\left(1-\frac{x}{R}\right)^{-1} = 1+\frac{x}{R}+\left(\frac{x}{R}\right)^2+\cdots$$

is also used, producing higher-order terms than that on the right-hand side of (6.30). Consequently, from (6.27), (6.29) and (6.30) we have

$$-\mathrm{i}G_0 = 2(\beta_0+\xi_0+\zeta_0), \tag{6.31}$$

if (6.22*a*) and (6.25) are equal.

After the first term of the expansion for G was found, the next-order terms in (6.29) and (6.30) can be pursued by substituting $G \approx G_0$ into (6.21), which will result in the terms of zeroth power of x in (6.29) and (6.30). These terms and the corresponding one in (6.27) as well as the $1/2R$ arising from the last term of (6.25), excluding those attributed to the series in (6.23), can be identified with $Q_0 \equiv Q(x=0)$ in (6.22*a*). This procedure can be continued to determine subsequent terms in the expansions for G and Q, and the results show that these expansions indeed take the form of a power series with its centre at $x=0$. Although there is no way to estimate the radii of convergence of these two series in a general situation, since the variation of the underlying current is slow, it is not unreasonable to anticipate that these series will be uniformly convergent in a large (compared with the wavelength) area centred at the caustic. Therefore we conclude that G, Q (and P) are regular at the caustic. This conclusion can also be drawn from a consideration of the action conservation equation for the reflected wave, because in this case, following the same procedure, one can obtain the same results except that the signs of the terms containing $\sqrt{\psi_1 x}$ in (6.27)–(6.30) become opposite, which also occurs to (6.22*b*) compared with (6.22*a*), so that the parameters G and Q in (6.22*b*) have the same values as those in (6.22*a*) and are indeed regular at the caustic.

In summary, by investigating the power-series expansion about the caustic and therefore the regularity at the caustic of each parameter in the equation and solutions, we have demonstrated that even for a curved moving caustic and for waves in an intermediate-depth region, the uniform asymptotic and the WKBJ solutions in the vicinity of the caustic take the same forms as those derived in Shyu & Phillips (1990) and in the preceding section. Since the existence of the series expansions is proved from the dispersion relation and the action conservation equation which themselves were deduced by Smith (1975) from the Laplace equation and the kinematical and dynamical boundary conditions, the present solutions are not independent of the dynamics. These solutions have provided explicit expressions for the amplitudes, although the Class 2 terms G and Q in them can be determined only numerically. This explicitness will in the next section prove of great use in a practical numerical computation of the reflection phenomenon.

7. An application to numerical computations

In this section, we shall conduct numerical simulations in two cases: a straight caustic and a curved caustic. Since it will later become clear that estimates of the reflected wave from the incident wave in the vicinity of the caustic at each instant involve only the instantaneous values of various variables and their derivatives with respect to x, and since the difference between n_1 and n_2 near a moving caustic is as small as that between k_{y1} and k_{y2} near a curved caustic (see the discussion following (6.14)), any conclusions drawn from the simulation of a curved caustic about the application of the present theory may have implications for the case of a moving caustic. To eliminate other complications without loss of generality, we also assume that all waves are in deep water.

Since we have in the earlier sections derived the analytical solutions, including the expressions for the Class 2 terms, in the case when a straight caustic is caused by a deep-water gravity wave propagating obliquely upon a steady unidirectional current, the results of the present numerical computations for this case can be compared with the analytical solutions to show the accuracy of the numerical schemes applied in cases of both a straight and a curved caustics. To achieve this purpose, even for a straight caustic, we deliberately take the directions (denoted by x' and y') of the computational grid not along $\boldsymbol{U}$ so that no simplifications which may originally be suitable to this special case will be made and the extension of the numerical model to the case of a curved caustic is straightforward. Also we note that although the analysis in the preceding section was made in a curvilinear coordinate system, without a prior knowledge of the location of the caustic, the differential equations can be solved numerically only on a rectangular grid for the incident wave, after which and after the caustic was determined numerically, the components of each vector relative to the curvilinear coordinate system defined in §6 can be calculated from those referred to (x', y'), and the results will be utilized to determine the reflected wave in the vicinity of the caustic.

Determination of the incident wave and the caustic

Since in the present simulations the underlying currents are steady, the action conservation equation can be reduced to

$$\frac{\partial}{\partial x'}\left[(U_{x'} + C_{gx'})\frac{a^2}{\sigma}\right] + \frac{\partial}{\partial y'}\left[(U_{y'} + C_{gy'})\frac{a^2}{\sigma}\right] = 0, \tag{7.1}$$

and the apparent frequency n remains constant (denoted by n_0 again) everywhere so that the wavenumber components $k_{x'}$ and $k_{y'}$ can be determined entirely from the irrotationality

$$\frac{\partial k_{y'}}{\partial x'} - \frac{\partial k_{x'}}{\partial y'} = 0 \tag{7.2}$$

and the dispersion relation

$$n_0 = \left[g\left(k_{x'}^2 + k_{y'}^2\right)^{1/2}\right]^{1/2} + U_{x'}k_{x'} + U_{y'}k_{y'}. \tag{7.3}$$

The partial differential equations (7.1) and (7.2) were solved by using a finite difference scheme, and (7.3) by using the Secant Method. These calculations can be made straightforwardly until at a certain point, the subroutine for the Secant Method fails to return a reliable and real root of (7.3) for $k_{x'}$ or $k_{y'}$, signifying the occurrence of the blockage phenomenon at this point. If this occurs at point A in figure 3, the solution values at the points on the same row and on the right side of A can still

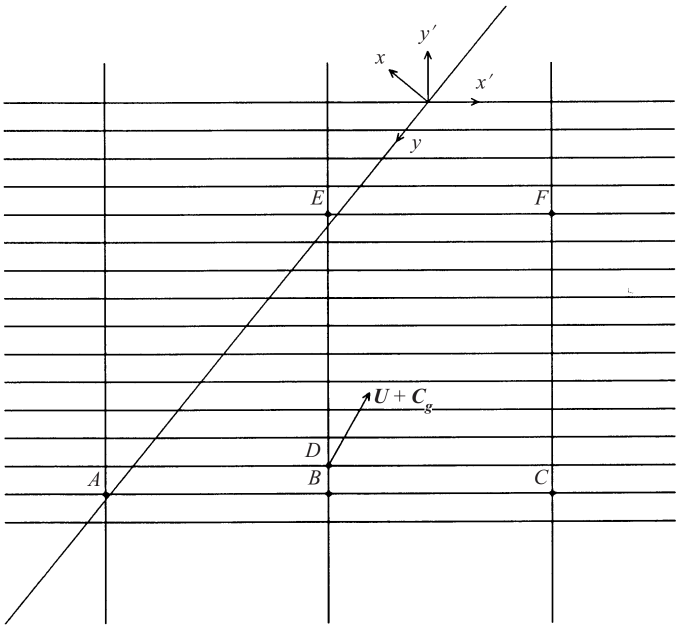

FIGURE 3. A diagram for illustration of the strategy to locate the caustic and compute the incident wave near the caustic.

be pursued. However, since point A is excluded from the integration domain, the solution of (7.1) at point D can be estimated only from the solution values at B and C, which violates the Courant–Friedrichs–Lewy (CFL) condition for the stability of the finite difference scheme, because near the caustic the characteristic velocity $\boldsymbol{U}+\boldsymbol{C}_g$ is almost tangent to the caustic so that the characteristic curve through D of equation (7.1) will meet the line AC at a point between A and B instead of between B and C (see figure 3). On the other hand, the values of $k_{x'}$ and $k_{y'}$ at point D can be calculated from those at B and C because the equations (7.2) and (7.3) represent a degenerate hyperbolic system in which all directions are formally characteristic (see Whitham 1974, § 5.1). Therefore the calculations of $\boldsymbol{k}$ (but not a) can be continued beyond the row containing A until the Secant Method fails again or U_x+C_{gx} becomes negative at another point, E say, which always occurs in the column next to point A. Consequently, the line AE in figure 3 can approximate the true caustic satisfactorily if the grid spacing in the y'-direction $\Delta y'$ is sufficiently small (for this reason, we have chosen $\Delta y' = 0.0625$ cm while $\Delta x' = 20$ cm in simulations of both a straight and a curved caustic). Note that $U_x + C_{gx}$ here represents the component of $\boldsymbol{U}+\boldsymbol{C}_g$ in the direction perpendicular to the estimate caustic.

After the caustic at point E was decided, the solution value a of equation (7.1) at point F can be calculated reliably by using the solution values at points B and C. This finite difference equation has a larger value of $\Delta y'$ but can however fulfil the CFL condition, because this time the characteristic curve through F of equation (7.1) will meet the line AC at a point between B and C as the characteristic velocity $\boldsymbol{U}+\boldsymbol{C}_g$ of the incident wave at points B and F always has a component towards the caustic (see figure 3). The numerical solution of a at the rest of the points on the same row as point F can be calculated without difficulty by using the solution values at the points on the same row as points B and C. Therefore we now have all the information required for a repetition of the above procedure to determine the next

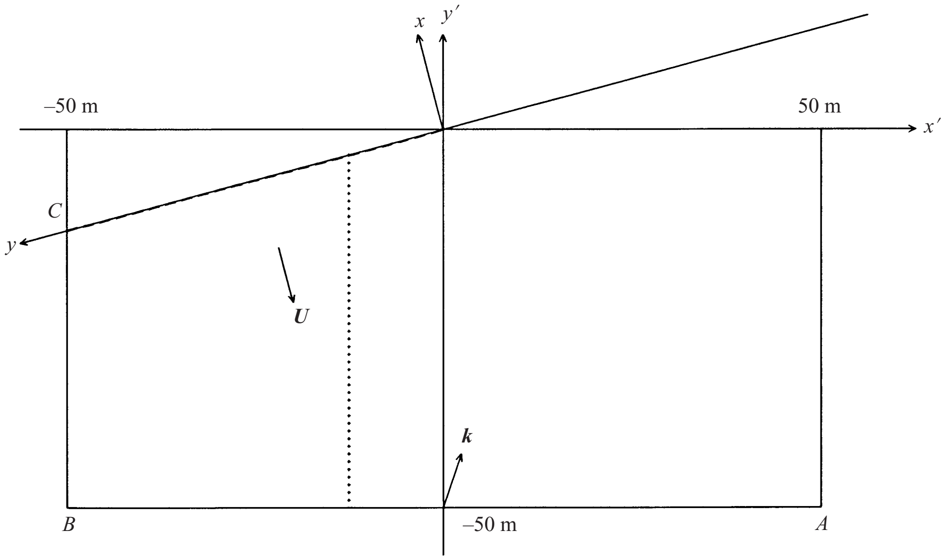

FIGURE 4. The domain of integration and the true (y-axis) and predicated (dashed line) locations of the caustic in the simulation of a straight caustic.

position of the caustic and calculate the solution values of the incident wave on that row.

The above strategy for estimates of the location of the caustic can be justified directly by a comparison between its numerical and analytical solutions in the case of a straight caustic (an indirect justification for the case of a curved caustic will also be given later). In this case, the conditions for the incoming wave prescribed on the boundaries AB and BC in figure 4 are determined from the requirements that $k_y = -0.94\,\mathrm{rad\,m^{-1}}$, $n_0 = 3.62\,\mathrm{rad\,s^{-1}}$, the component of the action flux in the x-direction is equal to $0.0625\,\mathrm{kg\,m\,s^{-2}}$ everywhere, and the velocity components of the underlying current

$$U_x = -0.6882 - 0.0077x\,\mathrm{m\,s^{-1}}, \qquad U_y = 0. \tag{7.4}$$

In this situation, one may easily prove that $k_x = 4.9\,\mathrm{rad\,m^{-1}}$ and $C_{gx} = 0.6882\,\mathrm{m\,s^{-1}}$ at $x = 0$, so that the y-axis represents the true caustic. Therefore, figure 4 indicates that by using the above strategy, the estimated caustic closely coincides with the true caustic.

On the other hand, to simulate the calculations for a curved caustic, we assume that the streamlines of the underlying larger-scale current are circles and the magnitude of the velocity at each point

$$|U| = -4.0\frac{3\pi/2 - \theta}{\pi}\frac{100}{r}\,\mathrm{m\,s^{-1}},$$

where (r, θ) represents the polar coordinates of this point (see figure 5). This velocity distribution has zero vorticity everywhere except at the point $r = 0$, which represents a singular point but will be excluded from the integration domain because of the wave blockage phenomenon. Another feature of this distribution is that when r is very large, $|U|$ becomes vanishingly small. Therefore a uniform deep-water wave train with frequency $n_0 = 1.7\,\mathrm{rad\,s^{-1}}$ propagating in a single direction can be prescribed on the boundaries AB and BC in figure 5 which are very far from the origin. From

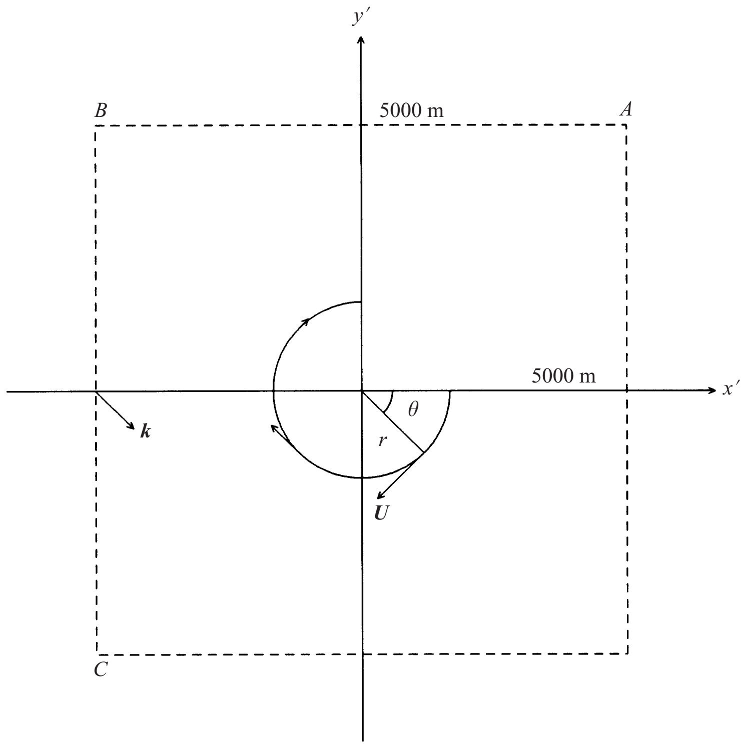

FIGURE 5. The domain of integration and the directions of the incoming wave and the current field in the simulation of a curved caustic.

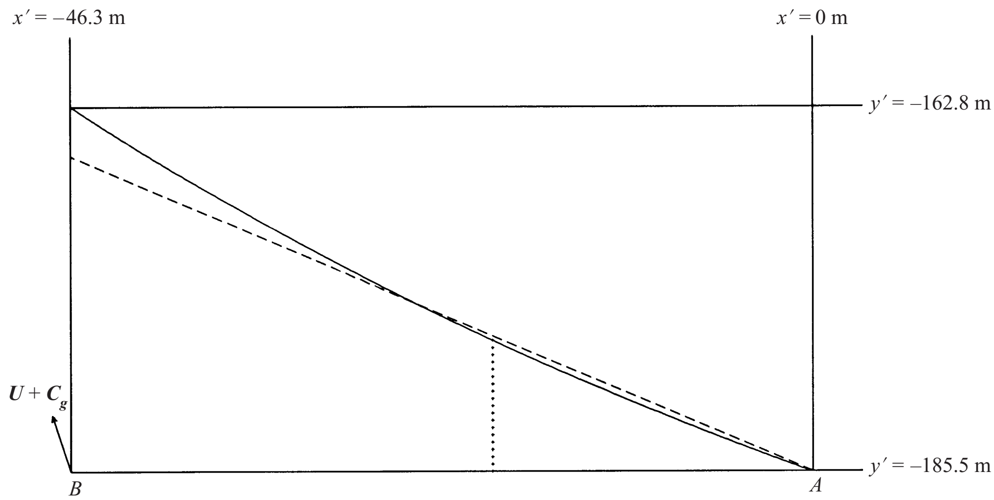

FIGURE 6. A part of the integration domain in figure 5 in which the caustic (solid curve) is located and the reflected wave estimated.

these boundary conditions and by using the numerical scheme, the variation of the wavenumber of the incident wave in the integration domain was solved until a blockage point (A, say) was first met. After this, the calculations were restricted to within the much smaller area specified in figure 6, in which the blockage point A had

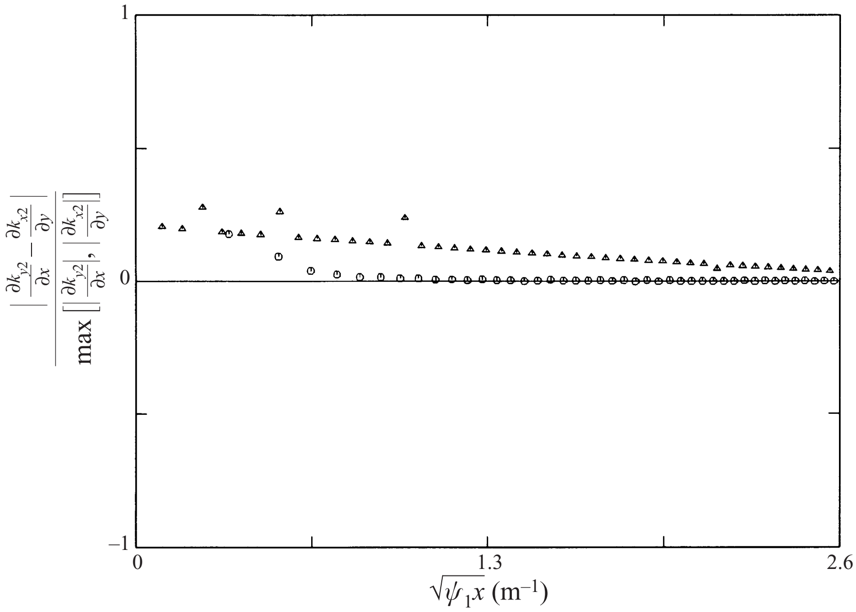

FIGURE 7. Dimensionless vorticity of the estimated wavenumbers of the reflected waves in the simulations of a straight caustic (circles) and a curved caustic (triangles).

been located and the numerical solutions of the wavenumber components at each point on line AB had also been estimated. Thus, to calculate the wavenumber as well as the amplitude of the incident wave in this small area, it is only necessary to prescribe the value of a_1 at each point on line AB in figure 6. In consideration of (6.21) and (6.15), the particular boundary condition of a_1 chosen here is

$$a_1 = (-\hat{x})^{-1/4}$$

where $-\hat{x}$ represents the distance from each point on AB to the dashed straight line in figure 6 which approximates the estimated caustic. Note that since a slowly modulated incoming wave is allowed by the theories, the above arrangement is convenient for development and tests of the present algorithm for estimates of the reflected wave in the vicinity of the caustic. Before these, the amplitude and wavenumber of the incident wave, including the location of the caustic, in the integration domain in figure 6 were estimated by using the above schemes and strategy. The resulting caustic as shown in figure 6 is indeed curved.

Determination of the reflected wave

After the incident wave field and the position of the caustic were determined, we proceeded to estimate the reflected wave in the vicinity of the caustic using Smith's (1975) theory and the present theory. The results can serve as the boundary conditions for calculations of the reflected wave in the regions away from the caustic.

Since the difference between k_{y1} and k_{y2} is very small near a curved caustic (see the note following (6.14)) and is zero in the case of a straight caustic, we let $k_{y2} = k_{y1}$ at each point in the vicinity of the caustic and then calculate the value of k_{x2} as another root of equation (7.3) which coalesces with k_{x1} at the caustic. The accuracy of these estimates can more or less be seen from a calculation of vorticity of the resulting $\boldsymbol{k}_2$ as shown in figure 7. (In this figure and in the following figures, the results presented are along the dotted lines in figures 4 and 6 for the cases of a straight and a curved caustic respectively, and also the values of $\sqrt{\psi_1 x}$ estimated from (6.15) by neglecting the higher powers of x are chosen as the abscissae of these figures.) The results in figure 7 indicate that the irrotationality is approximately fulfilled by the estimates of $\boldsymbol{k}_2$ in the case of a curved caustic and this fulfillment is even more satisfactory in the case of a straight caustic as might be expected.

Next, we shall calculate a_2 in terms of a_1 in the vicinity of the caustic by using Smith's (1975) theory. According to Smith (1975), the flux of wave action normal to the caustic carried by the incident and reflected waves is equal and opposite at the caustic, so that we have

$$\left[(U_x + C_{gx1})\frac{a_1^2}{\sigma_1}\right]_{x=0} = -\left[(U_x + C_{gx2})\frac{a_2^2}{\sigma_2}\right]_{x=0}. \tag{7.5}$$

Also integration with respect to x of (6.24) and of the corresponding equation for the reflected wave and substitution of (6.1) yield

$$\left.\begin{aligned}\left(1-\frac{x}{R}\right)\left[(U_x + C_{gx1})\frac{a_1^2}{\sigma_1}\right] - \left[(U_x + C_{gx1})\frac{a_1^2}{\sigma_1}\right]_{x=0} &= \int_0^x F_1(x,y,t)\,\mathrm{d}x,\\ \left(1-\frac{x}{R}\right)\left[(U_x + C_{gx2})\frac{a_2^2}{\sigma_2}\right] - \left[(U_x + C_{gx2})\frac{a_2^2}{\sigma_2}\right]_{x=0} &= \int_0^x F_2(x,y,t)\,\mathrm{d}x,\end{aligned}\right\} \tag{7.6}$$

where

$$\left.\begin{aligned}F_1 &= -\left(1-\frac{x}{R}\right)\frac{\partial}{\partial t}\left(\frac{a_1^2}{\sigma_1}\right) - \frac{\partial}{\partial y}\left[(U_y + C_{gy1})\frac{a_1^2}{\sigma_1}\right],\\ F_2 &= -\left(1-\frac{x}{R}\right)\frac{\partial}{\partial t}\left(\frac{a_2^2}{\sigma_2}\right) - \frac{\partial}{\partial y}\left[(U_y + C_{gy2})\frac{a_2^2}{\sigma_2}\right].\end{aligned}\right\} \tag{7.7}$$

From (6.25) and by virtue of (6.27), (6.29) and (6.30), it is clear that F_1 and F_2 are of secondary importance to the variations of a_1 and a_2 respectively in the vicinity of the caustic. Therefore it is only required to estimate the first approximations of F_1 and F_2 in this region, which can be written as

$$F_1 \approx F_2 \approx \frac{\tau_0}{\sqrt{\psi_1 x}} \tag{7.8}$$

in view of (6.28)–(6.30) and due to the fact that each of a, σ and $U_y + C_{gy}$ for the incident wave has the same one-term approximation as that for the reflected wave in the vicinity of the caustic. Thus, substituting (7.5) and (7.8) into (7.6) and carrying out the integration and combination, we obtain

$$\left[(U_x + C_{gx2})\frac{a_2^2}{\sigma_2}\right] \approx -\left[(U_x + C_{gx1})\frac{a_1^2}{\sigma_1}\right] + 4\frac{\tau_0}{\psi_1}\sqrt{\psi_1 x} \tag{7.9}$$

at each point in the vicinity of the caustic. In (7.9), the terms containing the radius of curvature R of the caustic are of higher powers of x than the last term so that they were neglected consistently. On the other hand, it can be shown with equations (6.26) and (6.28) that the last term in (7.9) has the same power of x as the second terms in the series expansions of the two major terms in (7.9), and should therefore be taken into account in a general situation as the first terms of these series predict that $a_2/a_1 = 1$ and $(U_x + C_{gx1})/\sigma_1 = -(U_x + C_{gx2})/\sigma_2$ in the vicinity of the caustic, which are certainly insufficient. The relations (7.7)–(7.9) together indicate that the ratio a_2/a_1 at each grid point near the caustic can in theory be estimated from the solution values of a_1, k_1 and k_2 obtained earlier. Also we emphasize that since the coefficients of the higher powers of x in the series expansion of a slowly varying parameter are proportional to its higher-order derivatives and therefore are smaller, the approximation (7.9) can be very accurate even for a moderate value of x. A similar situation will also occur in the application of the present theory.

When the present theory is under consideration, from (6.21) and (6.17) it immediately follows that

$$\frac{a_2}{a_1} = \exp\left[\int_0^x \mathrm{i}G/H^{1/2}\,\mathrm{d}x\right] \approx \exp\left[-2\mathrm{i}G_0(-\psi_1)^{-1/2}(-x)^{1/2}\right]. \tag{7.10}$$

Since

$$\exp\left[-2\mathrm{i}G_0(-\psi_1)^{-1/2}(-x)^{1/2}\right] \approx 1 - 2\mathrm{i}G_0(-\psi_1)^{-1/2}(-x)^{1/2}, \tag{7.11}$$

it is clear that the parameter G_0 (or strictly speaking, $-\mathrm{i}G_0(-\psi_1)^{-1/2}$) is closely related to the difference between the amplitudes of the incident and reflected waves in the vicinity of the caustic. From (6.22*a*, *b*) and (6.15), we also have

$$\frac{a_2'}{a_2} - \frac{a_1'}{a_1} = \mathrm{i}G/H^{1/2} \approx \mathrm{i}G_0/\sqrt{\psi_1 x} \tag{7.12}$$

so that the value of $-\mathrm{i}G_0(-\psi_1)^{-1/2}$ can be estimated from the solutions of a_1'/a_1 and a_2'/a_2, which themselves can be calculated respectively from (6.25) and from the corresponding equation for a_2'/a_2 as follows.

The first terms on the right-hand side of equation (6.25) and on that of the corresponding equation for a_2'/a_2 can be computed solely from the numerical solutions of $\boldsymbol{k}_1$ and $\boldsymbol{k}_2$ respectively. On the other hand, the one-term approximations of the second and third terms on the right-hand side of (6.25) are equal in magnitude and opposite in sign to those of the corresponding equation for a_2'/a_2 in view of (7.8) and (7.5). Therefore, even without solving (7.1) for a_2, the approximation of a_2'/a_2 at each point near the caustic can still be estimated, so that the value of $-\mathrm{i}G_0(-\psi_1)^{-1/2}$ in (7.12) and eventually the values of a_2/a_1 in (7.10) in the vicinity of the caustic can be calculated in theory. Notice that the last terms in (6.25) and in the corresponding equation for a_2'/a_2 are equal to each other and therefore are cancelled out from (7.12).

Figure 8 shows the estimates of a_2/a_1 using Smith's (1975) theory and the present theory in the simulation of a straight caustic, which coincide with each other closely. However, to make sure that no common errors (e.g. the discretization errors) have occurred to both estimators, in figure 8 we also show a_2/a_1 calculated directly from the expression

$$\frac{a_2}{a_1} = \left[-\frac{(U_x + C_{gx1})\sigma_2}{(U_x + C_{gx2})\sigma_1}\right]^{1/2} \tag{7.13}$$

in which the values of $\sigma_1, \sigma_2, C_{gx1}$ and C_{gx2} at each point were determined simply by substitution of $k_y = -0.94\,\mathrm{rad\,m^{-1}}$ and $n_0 = 3.62\,\mathrm{rad\,s^{-1}}$ into the dispersion relation (2.2). The results in figure 8 indicate that the present numerical schemes with sufficiently small grid spacings are indeed very accurate (the deviation of the curve in figure 8 from a straight line near its left end is due to the errors in the estimates of $\sqrt{\psi_1 x}$ instead of a_2/a_1).

In figure 9 we compare the numerical solutions of $-\mathrm{i}G_0(-\psi_1)^{-1/2}$ and Q_0 with their

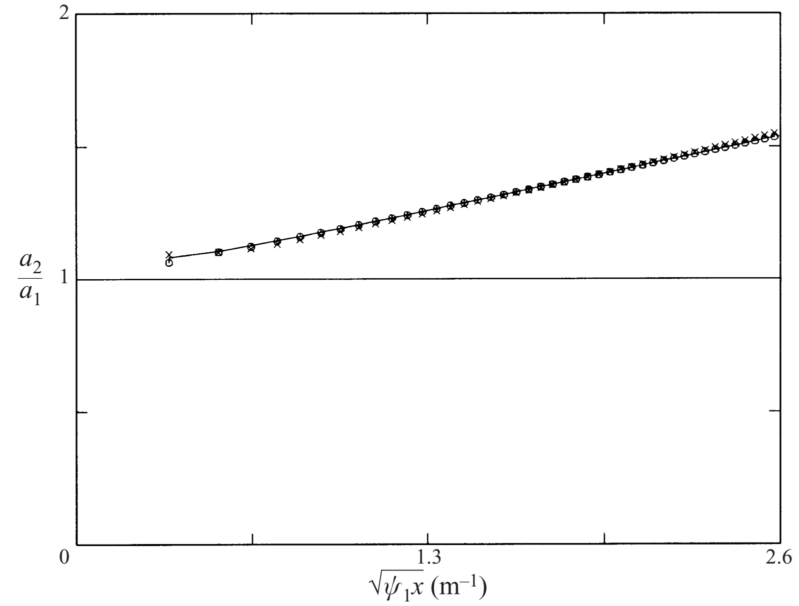

FIGURE 8. Estimates of a_2/a_1 by using Smith's (1975) theory (⊙) and the present theory (×) in the simulation of a straight caustic. The curve represents the true values calculated from (7.13).

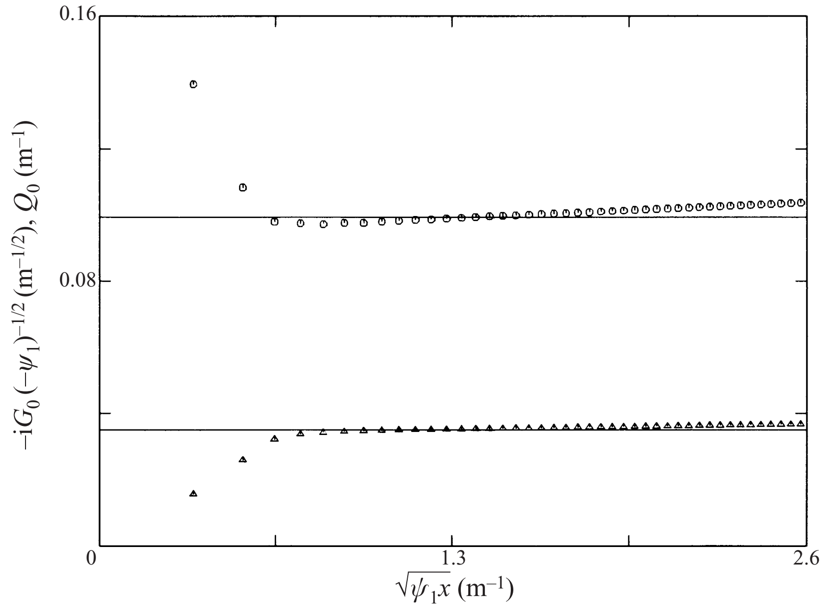

FIGURE 9. Estimates of $-iG_0(-\psi_1)^{-1/2}$ (circles) and Q_0 (triangles) in the simulation of a straight caustic by using (7.12) and (7.14) respectively and comparisons with their analytical solutions (horizontal lines).

analytical solutions derived in §§4 and 5, while the numerical solution of Q_0 was calculated by using the relation

$$Q_0 \approx -2\frac{a_1'}{a_1} - i\frac{G_0}{\sqrt{\psi_1 x}} - \frac{k_{x2}' - k_{x1}'}{k_{x2} - k_{x1}} \tag{7.14}$$

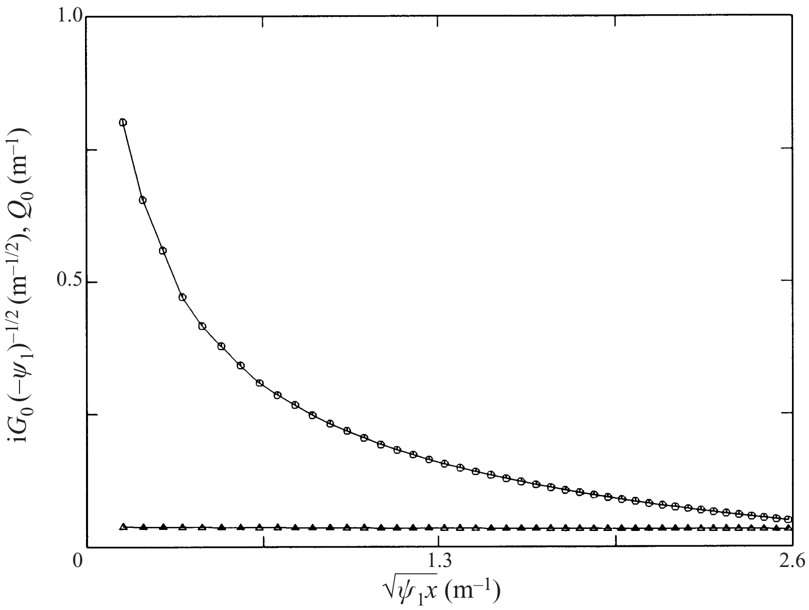

FIGURE 10. Estimates of $iG_0(-\psi_1)^{-1/2}$ (circles) and Q_0 (triangles) in the simulation of a curved caustic by using (7.12) and (7.14) respectively.

by virtue of (6.22*a*) and (6.15). The results in figure 9 are very satisfactory except that, in the immediate vicinity of the caustic, the numerical schemes have produced significant errors owing to the singularities of a_1, $\boldsymbol{k}_1$ and $\boldsymbol{k}_2$ at the caustic. This comparison has provided a valuable check on the expressions for the Class 2 terms, including (4.6) for ψ_1, which are available only for a straight caustic.

In the simulation of a curved caustic, this comparison is not feasible because of the absence of these expressions. However, when (7.9) was utilized to estimate a_2/a_1 in this case, it was found that the values of $(a_2/a_1)^2$ at all points in the vicinity of the caustic became negative, which is impossible, meaning that significant errors have occurred in the estimates. On the other hand, when the present theory was applied, especially when (7.12) was invoked, the values of $-iG_0(-\psi_1)^{-1/2}$ also became negative and in addition, they were far from being constant (see figure 10). Therefore it is evident that in the simulation of a curved caustic, if the relation (7.12) is invoked, large errors also will occur in the application of the present theory to estimate a_2/a_1.

To identify the sources of these errors, figure 11 exhibits the estimates of a_1'/a_1 using (6.25), together with those of the first term (denoted by $\overline{a_1'/a_1}$) on the right-hand side of (6.25), which indicate that at each point, the difference between the estimates of a_1'/a_1 and $\overline{a_1'/a_1}$, which represents the estimate of the third term on the right-hand side of (6.25) in the present simulation, has the same order of magnitude as a_1'/a_1. This is inconsistent with the theory that in the vicinity of the caustic the third term on the right-hand side of (6.25) is one order (in terms of $x^{1/2}$) smaller than the first term (cf. (6.27) and (6.30)). In figure 11, we also show the solution values of a_1'/a_1 determined directly from numerical differentiation of a_1 obtained earlier, indicating that except in the region very near the caustic, these values coincide closely with the estimates of a_1'/a_1 using (6.25). Furthermore, these two sets of estimates for a_1'/a_1 are also close to the values of the leading term $-1/4x$ in the series expansion of $\overline{a_1'/a_1}$ (see (6.27)), which

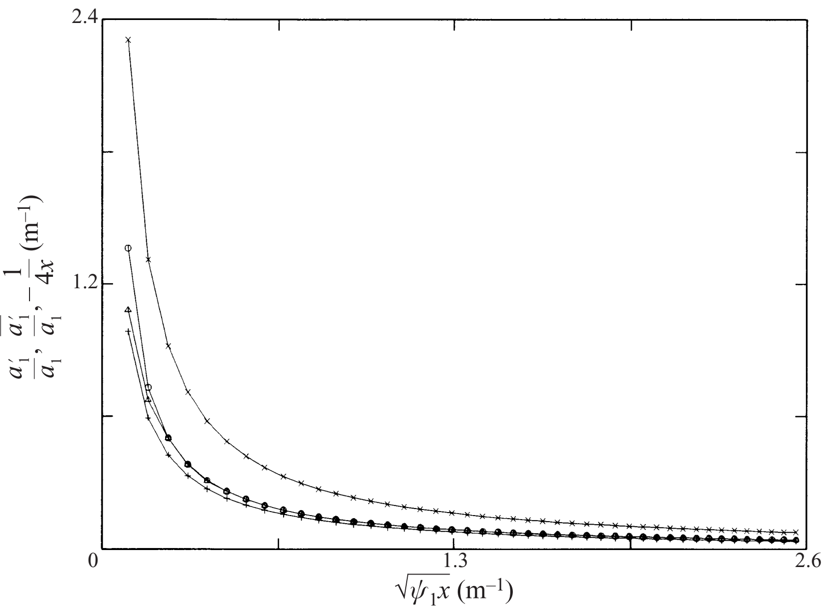

FIGURE 11. Comparisons between two kinds of estimates of a_1'/a_1 and between a_1'/a_1 and $-1/4x$ (+). The circles and the triangles are the estimates of a_1'/a_1 obtained respectively from numerical differentiation of a_1 and from summation of the estimates of $\overline{a_1'/a_1}$ (×) and (6.30).

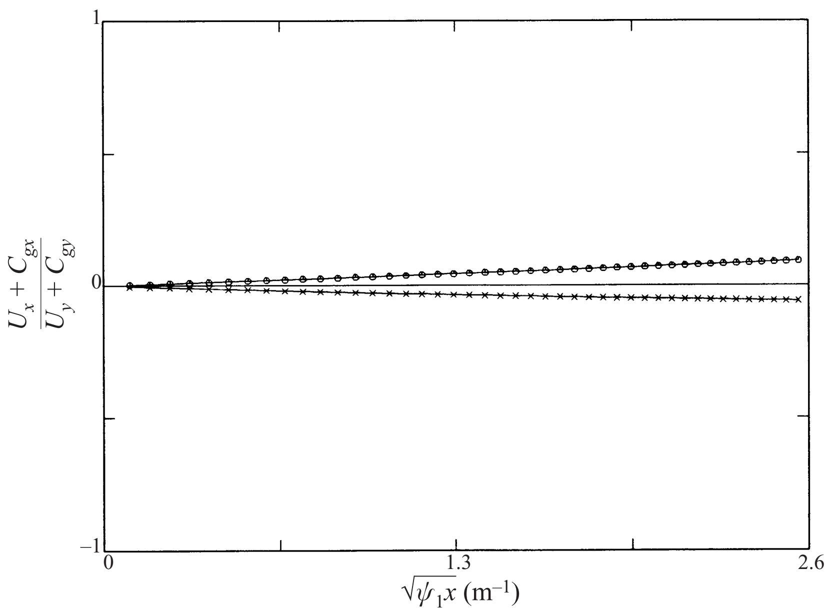

FIGURE 12. Values of $(U_x + C_{gx})/(U_y + C_{gy})$ of the incident (⊙) and reflected (×) waves in the simulation of a curved caustic.

are also shown in figure 11. All of this leads us to believe that the significant errors mentioned above are mainly due to misalignment of the curvilinear coordinate lines.

Since in the vicinity of the caustic, the absolute values of $U_x + C_{gx1}$ and $U_x + C_{gx2}$ are small (recall that $U_x + C_{gx1} = U_x + C_{gx2} = 0$ at the caustic) compared with those of $U_y + C_{gy1}$ and $U_y + C_{gy2}$ in the simulation of a curved caustic (see figure 12), very slight misalignment of the x-axis can cause large percentage changes in the estimates of $U_x + C_{gx1}$ and $U_x + C_{gx2}$ and therefore in the estimates of the first terms on the right-hand sides of (6.25) and of the corresponding equation for a_2'/a_2. On the other hand, since in the vicinity of the caustic, the absolute values of $\partial[(U_y + C_{gy1})a_1^2/\sigma_1]/\partial y$ are very small compared with those of $\partial[(U_y + C_{gy1})a_1^2/\sigma_1]/\partial x$ (both of which represent the components of a second-order tensor), slight misalignment of the coordinate lines can also produce very large percentage changes in the estimates of $\partial[(U_y + C_{gy1})a_1^2/\sigma_1]/\partial y$. These changes together with those in $U_x + C_{gx1}$ account for the disproportionately large changes in the third term on the right-hand side of (6.25). However, for those quantities (for example, a_1'/a_1 and $-1/4x$) which are insensitive to a slight rotations of the coordinate axes, their estimates, no matter which method is applied, will remain nearly unchanged under slight misalignment of the coordinate lines. This can explain why in figure 11 the sum of the estimates of the first and third terms on the right-hand side of (6.25), though each of them contains significant errors, coincides closely with the value of a_1'/a_1 obtained directly from numerical differentiation of a_1 which itself is the numerical solution of (7.1).

Since equation (7.1) was solved on a rectangular grid which is independent of the location of the caustic, and since $a_1' \equiv \partial a_1/\partial x \gg \partial a_1/\partial y$, slight rotation of the curvilinear coordinate lines obviously has no effect on the solution values of a_1 and has only a very small effect on the estimates of a_1'/a_1 obtained straightforwardly from numerical differentiation of a_1. Therefore the estimates of a_1'/a_1 in figure 11 should be very accurate, except that in the immediate vicinity of the caustic large discretization errors may occur due to the singularities at the caustic. Incidentally, the small differences between a_1'/a_1 and $-1/4x$ in figure 11 provide evidence that the position of the curved caustic (from which the values of x were measured) had been located accurately.

From the above discussion it is clear that in the vicinity of a curved caustic, all terms on the right-hand side of (6.25), except the last and less important term, cannot be estimated individually, meaning that the strategies described above to estimate the last term in (7.9) and the term a_2'/a_2 in (7.12) will fail in general. Even if the divergence of the action flux in the y-direction and the local rate of change of wave action are negligible, since the quantities $[-(U_x + C_{gx1})/\sigma_1]/[(U_x + C_{gx2})/\sigma_2]$, $\overline{a_1'/a_1}$ and $\overline{a_2'/a_2}$ cannot be estimated reliably, it is still impossible to estimate a_2/a_1 through (7.9) or through (7.10) and (7.12). This situation will certainly become less severe in the regions far away from the caustic; however in these regions the third term on the right-hand side of (6.25) can hardly be negligible in the case of a curved caustic, and in the meantime the one-term approximations given in (7.8), (7.10) and (7.12) and in the estimates of a_2'/a_2 may become inappropriate. On the other hand, although the approximation $a_2/a_1 \approx 1$ can be accurate enough in the immediate vicinity of the caustic, the estimates of a_1 themselves in this region may contain significant errors due to the fact that a_1 and $\boldsymbol{k}_1$ are singular at the caustic. Besides, when the caustic is curved and the reflected wave field is still solved on a rectangular grid for convenience, it is often required to determine the boundary conditions of the reflected wave at the grid points with diverse values of x. As a consequence, the approximation $a_2/a_1 \approx 1$ cannot be applied equally well on these points. Therefore another effort should be made to avoid the error magnification phenomenon.

Since both a_1'/a_1 and $1/4x$ can be estimated accurately and from (6.22*a*), (6.23) and (6.15) we have

$$-\frac{\mathrm{i}G_0}{2\sqrt{\psi_1 x}} \approx \frac{a_1'}{a_1} + \frac{1}{4x}, \tag{7.15}$$

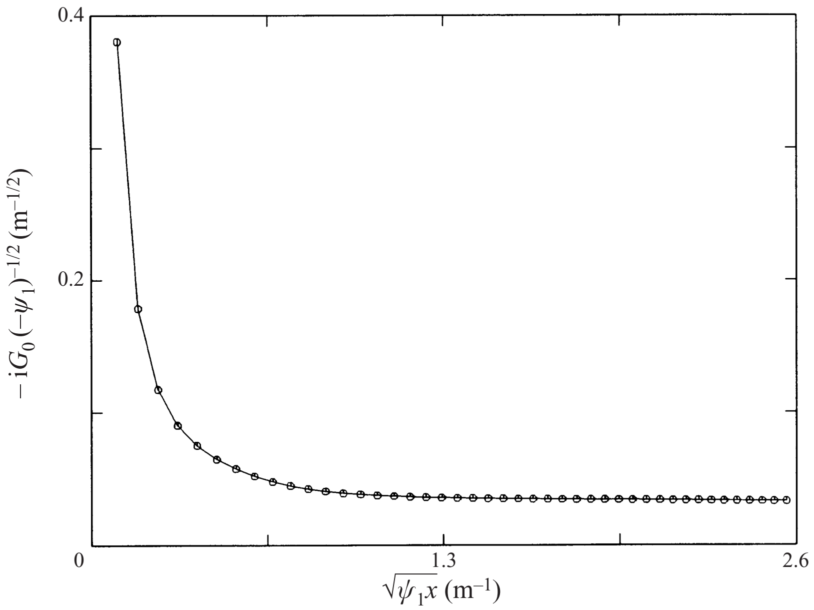

FIGURE 13. Estimates of $-\mathrm{i}G_0(-\psi_1)^{-1/2}$ by using (7.15) in the simulation of a curved caustic.

the approximation of $-\mathrm{i}G_0(-\psi_1)^{-1/2}$ can therefore be estimated reliably from this relation. By substitution of this value into (7.10), we may finally obtain the approximation of a_2/a_1 at each point in the vicinity of the caustic.

In (7.15) the zeroth power of x has been neglected which in (7.12) is completely cancelled out. This cancellation also occurs to the first power of x in (7.9). Therefore it seems that the estimates of $-\mathrm{i}G_0(-\psi_1)^{-1/2}$ by using (7.15) represent a lower-order approximation than those by using (7.12), but this is true only if the second and third terms on the right-hand side of (6.25) are vanishingly small, otherwise the estimates of a_2'/a_2 in (7.12) and $(4\tau_0/\psi_1)\sqrt{\psi_1 x}$ in (7.9) using the method described above will introduce the truncation errors of the zeroth and first powers of x respectively, because of the use of the one-term asymptotic approximations in this method. Hence, in a general situation, even without consideration of the error magnification phenomenon, it is still impossible to achieve the same accuracy as that shown in figures 8 and 9 for a straight caustic, although one may expect that the truncation errors in (7.15) will decrease if the modulation rates of the current field get progressively smaller. Nevertheless, even in the present simulation of a curved caustic, since the error magnification phenomenon has mostly been avoided in the application of (7.15), the resulting estimates of $-\mathrm{i}G_0(-\psi_1)^{-1/2}$ in figure 13 approach a constant far more satisfactorily than those in figure 10.

Since the true value of $-\mathrm{i}G_0(-\psi_1)^{-1/2}$ in figure 13 is unknown, for a comparison between the numerical and analytical solutions, we also estimated $-\mathrm{i}G_0(-\psi_1)^{-1/2}$ by using (7.15) in the simulation of a straight caustic. The results in figure 14 indicate that the new estimates of $-\mathrm{i}G_0(-\psi_1)^{-1/2}$, though less accurate than those in figure 9, can fit the analytical solution to within 25%. Therefore, if the true value of a_2/a_1 at a certain point is 1.25, then neglect of the exponent in (7.10) produces a relative error of 20% in a_2/a_1, but this figure can be reduced to about 5% by an application of the present theory.

After the approximation of a_2/a_1 (and therefore a_2) at each point in the vicinity of

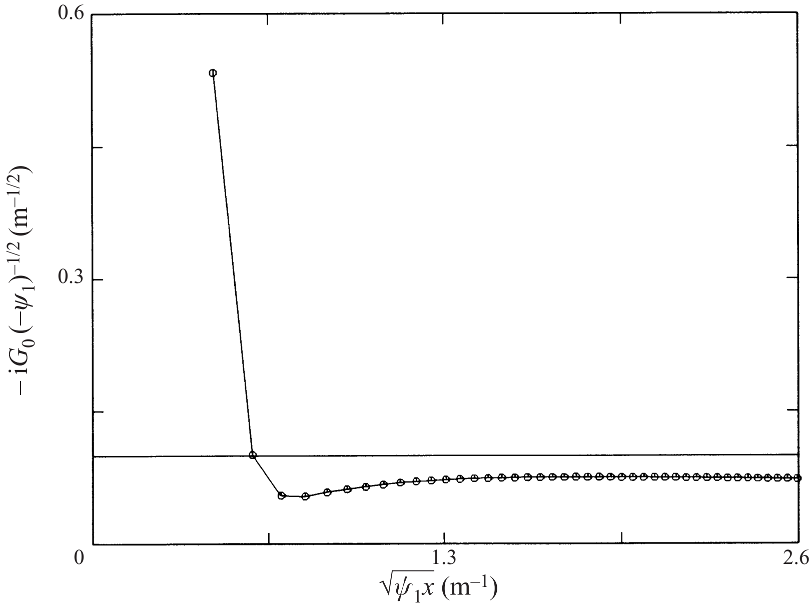

FIGURE 14. Estimates of $-\mathrm{i}G_0(-\psi_1)^{-1/2}$ by using (7.15) in the simulation of a straight caustic. The horizontal line represents the analytical solution.

the caustic has been determined, these values and the values of $\boldsymbol{k}_2$ in the same region obtained earlier can serve as the boundary conditions for calculations of the reflected wave in the regions away from the caustic. This task is just routine and therefore requires no elaboration here.

8. The wave profiles near caustics

The algorithm proposed above to estimate the parameters in the present solutions for a curved moving caustic will leave the parameter Q_0 unsolved (since the equation (7.14) and its approximation (7.15) cannot be applied to the estimates of both Q_0 and $-\mathrm{i}G_0(-\psi_1)^{-1/2}$); even G_0 and ψ_1 cannot be determined individually with this algorithm. For some problems these deficiencies are unimportant as long as the amplitude (and in some cases, the phase) of the reflected wave can be estimated with sufficient accuracy. However, in order to clarify the details of the wave profiles in the immediate vicinity of the caustic which might be intimately related to the abnormally large waves observed in areas of strong current, as suggested first by Peregrine (1976) and Smith (1976), it is worthwhile in this section to apply the analytical solutions derived in §5 for a straight caustic to the example described by (7.4) and by the statement above it. The results will then have implications for the case of a curved moving caustic as the forms of the solutions for both cases are pretty nearly the same.

In figure 15, three instantaneous profiles of the water surface at $t = 0$ along lines $y = 5.0\,\mathrm{m}$, $y = 6.6\,\mathrm{m}$ and $y = 8.2\,\mathrm{m}$ are computed by using the uniform solution (5.1), (5.5) and (5.6) and the WKBJ solution (5.12), while the properties of the incident and reflected waves specified explicitly by the latter are illustrated in figure 16. Note that since the WKBJ solution for $x \gg 0$ obtained by replacing $\mathrm{Ai}\,(-r)$ and $\mathrm{Ai}'\,(-r)$ in (5.5) with their asymptotic approximations for r large and negative cannot be separated

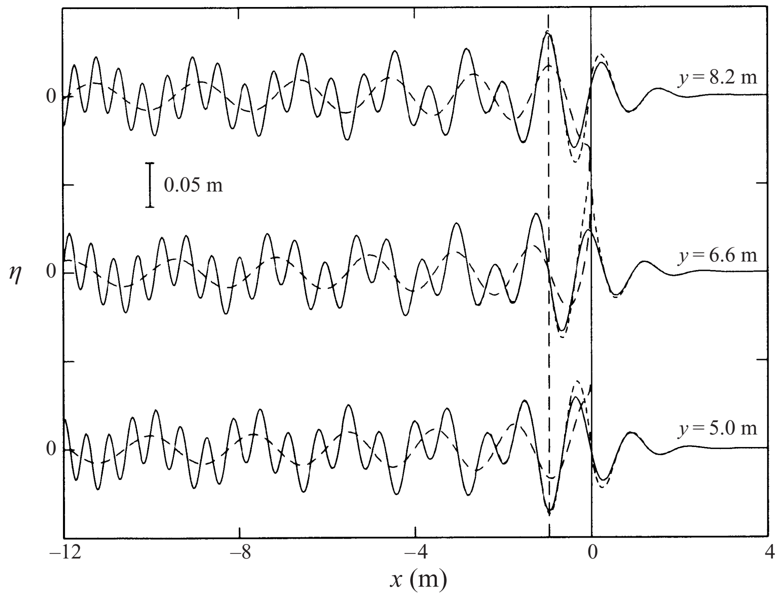

FIGURE 15. The instantaneous profiles of the water surface along lines y = const. in the simulation of a straight caustic. The solid curves represent the uniform solution, the short-dashed lines the WKBJ solution, and the long-dashed lines the incident wave component of the latter.

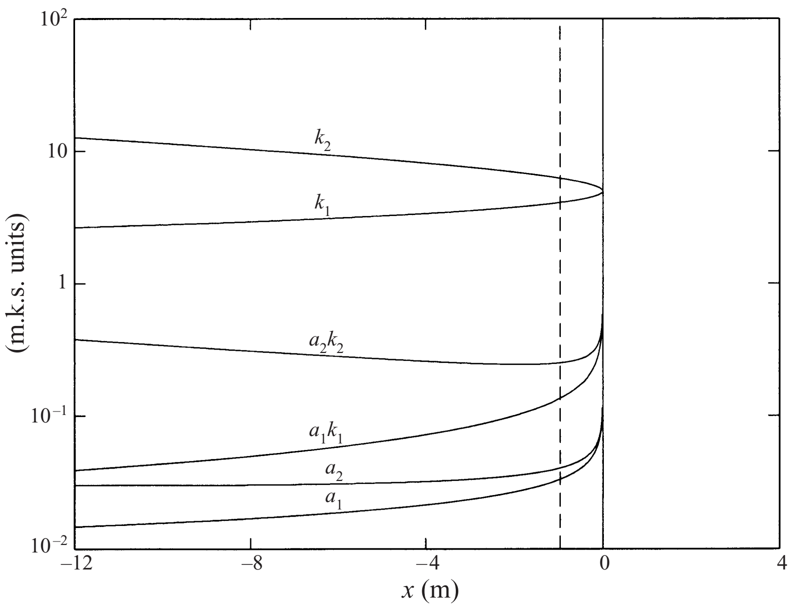

FIGURE 16. Variation of wavenumbers, slopes and amplitudes of the incident and reflected waves in the simulation of a straight caustic.

into two parts corresponding to the incident and reflected waves respectively, the wave properties in the region $x > 0$ have not been shown in figure 16.

In figure 15, the WKBJ solution fits the uniform solution very well in the regions away from the caustic as expected. Even in the immediate vicinity of the caustic,

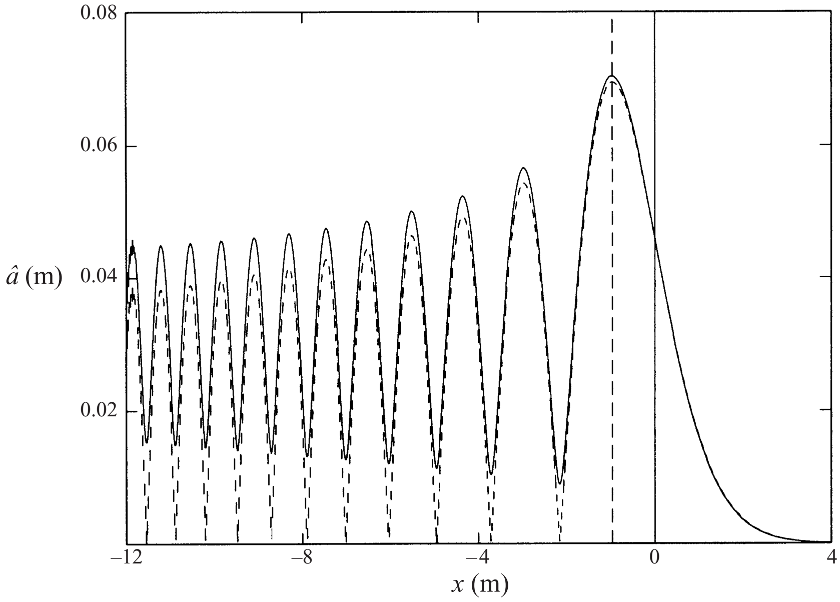

FIGURE 17. Variation of $\hat{a}$ in the simulation of a straight caustic. The dashed line represents the absolute magnitude of Ai$(-r)$ (the relation between r and x is given by (5.6*a*)) multiplied by a constant to make the resulting quantity equal to $\hat{a}$ at the caustic $x = 0$.

the differences between these two solutions in the profiles at the top and bottom of figure 15 are not so great as one might expect, but this is true only if $k_y y - n_0 t \approx \pi/2 \pm n\pi$, $n = 0, 1, 2, \ldots$ so that the surface displacement η represented by the real parts of (5.1) and (5.12) are both approximately equal to zero when $x \approx 0$. The differences between the values of y for the neighbouring profiles in figure 15 were chosen to be about one quarter of the wavelength in the y-direction $|2\pi/k_y| = 6.68$ m. However, the specific values y chosen here are such that at $t = 0$ and $x = 0.96$ m (marked by a broken vertical line in figures 15–17), the surface displacement η reaches the minimum at $y \approx 5.0$ m and the maximum at $y \approx 8.2$ m, and the amplitude of this variation is larger than that along any other line $x =$ const. Therefore figure 15 has shown the deepest trough and the highest crest in this region. Also we remark that since in the present case the roles played by the parameters k_y and n_0 in the solutions for η are similar to each other, the variation of η with y at a fixed time and a fixed value of x is analogous to that with time at a fixed position with the same value of x. Thus the wave profiles in figure 15 can also be interpreted as those occuring at three different instants but the same location.

The amplitude (denoted by $\hat{a}$) of the oscillation of the water surface at any fixed spatial point, including the blockage point, can easily be determined from the uniform solution (5.1) as its absolute magnitude. The results shown in figure 17 indicate that the value of $\hat{a}$ at $x = 0.96$ m is indeed larger than that at any other value of x, including that at the caustic $x = 0$. Another striking feature of the function $\hat{a}(x)$ is that the variation of $\hat{a}$ itself with x also exhibits oscillatory behaviour, similar to that found by Tung & Shyu (1992) in the variation (with frequency) of the frequency spectrum arising from a random wave train encountering an adverse current and reflected by it. This oscillatory behaviour is simply due to the fact that the incident wave and the reflected wave have the same observed frequency but different wavenumbers so that a superposition of them leads to an enhancement of $\hat{a}$ at some places but a reduction of it at others. Thus the largest value of $\hat{a}$ occurring at $x = 0.96$ m results from an enhancement of the amplitude to the highest degree by a superposition of the incident and reflected waves, each of which at $x = 0.96$ m has amplitude larger than that at any other peak in figure 17 according to figure 16. On the other hand, since the wavenumbers of the incident and reflected waves at $x = 0.96$ m are not very different from each other, the configuration of this highest individual wave resulting from a combination of the incident and reflected waves is not very distinct from a single progressive sinusoidal wave, as opposed to those waves at other peaks in figure 17, which as $|x|$ increases, have more and more the features of a short wave riding on a long wave (see figure 15). As a result, the profiles at the bottom of figure 15 exhibit a deep trough at $x = 0.96$ m, which associated with the subsequently arrived crest shown in the profiles at the top of figure 15 coincides with the description of freak waves given by Mallory (1974) as having a steeper forward face preceded by a deep trough, or 'hole in the sea'. These waves if high enough will present a special hazard to shipping as explained by Mallory (1974), Smith (1976) and White & Fornberg (1998).

The situation that $\hat{a}(x)$ features oscillatory behaviour and its highest peak is also the one closest to the caustic can also be attributed mathematically to the characteristics of the Airy function $\mathrm{Ai}\,(-r)$ occurring in the uniform solutions. This is because in the vicinity of the caustic, the coefficient C_0 of the term $\mathrm{Ai}'\,(-r)$ in (5.5) and in (6.6), which is mainly responsible for the amplitude of the reflected wave not being equal to that of the incident wave (see (5.6) and (6.8) and recall that $a_2/a_1 = 1$ if $\int_0^x G/H^{1/2}\,\mathrm{d}x = 0$), is smaller than the coefficient A_0 of $\mathrm{Ai}\,(-r)$ (for a more detailed and rigorous analysis of the orders of magnitude of these two terms, see Smith 1975 and Trulsen & Mei 1993). This and the fact that the coefficient A_0 and the factor $\exp\{-\int_0^x Q/2\,\mathrm{d}x\}$ in (5.1) and in (6.5) vary with x only slowly ensure that even in the case of a curved moving caustic, the chief features of $\mathrm{Ai}\,(-r)$ which also shown in figure 17, can be retained in the distribution of $\hat{a}$ in the vicinity of the caustic. Thus in cases of both a straight and a curved moving caustic with all possible values of H, G and Q, the highest peak of $\hat{a}(x)$ will always occur at a nearly fixed value of r which is dimensionless and is allied to the quantity $k_{x2} - k_{x1}$ through (6.7) and (6.9). Therefore, it is likely that the situation described in the preceding paragraph is general, so that in storm conditions, if this situation is not completely obscured by the finite-amplitude effects, freak waves will always occur in the caustic regions, as suggested first by Peregrine (1976) and Smith (1976).

9. Conclusions

When short deep-water gravity waves propagate obliquely upon a steady unidirectional irrotational current and are reflected by it, a second-order ordinary differential equation for the surface displacement of the short waves is derived from the Laplace equation and the kinematical and dynamical boundary conditions. This equation takes the same form as that derived by Shyu & Phillips (1990), although the expressions for the Class 2 terms in the coefficients of the present equation are much more complicated than those in Shyu & Phillips (1990). The regularity of this equation at the caustic is demonstrated and its uniform asymptotic solution and the corresponding WKBJ solution are subsequently derived. The satisfaction of the action conservation principle by this WKBJ solution at every point including the caustic has also been proved elsewhere.

Except for the expressions for the Class 2 terms, Shyu & Phillips' (1990) solutions and the present solutions take the forms valid even for waves in an intermediate-depth region and near a curved moving caustic induced by an unsteady multidirectional irrotational current. This suggestion is verified in a curvilinear coordinate system from considerations of the dispersion relation and the action conservation equation which themselves have been deduced by Smith (1975) in the vicinity of the caustic in exactly the same situation. In this general situation, the Class 2 term in the solutions which is responsible for the amplitude of the reflected wave being unequal to that of the incident wave in the vicinity of the caustic, can be estimated in a numerical calculation. The algorithm for this estimation is developed and tested in the numerical simulations of a straight and a curved caustic, but its validity in the case of a moving caustic is also obvious. The results of these simulations indicate that for a curved caustic, while the errors due to misalignment of the coordinate lines are magnified very seriously in the previous estimates of the amplitude of the reflected wave in the vicinity of the caustic from a consideration of the action conservation principle, this situation can be improved significantly by using the present algorithm.

The cause of the error magnification phenomenon is that when the component (such as $U_x + C_{gx1}$ in (7.9)) of a vector involved in the application of the action conservation principle to estimate a_2/a_1 is much smaller than another component of this vector in the vicinity of the caustic, very slight misalignment of the curvilinear coordinate lines will produce large percentage changes in this small component and consequently in the estimates of a_2/a_1. This situation can be avoided in the application of (7.15) to estimate the Class 2 term $-\mathrm{i}G_0(-\psi_1)^{-1/2}$ and eventually the values of a_2/a_1 in the vicinity of the caustic by using (7.10), because in this region $a_1' \equiv \partial a_1/\partial x \gg \partial a_1/\partial y$ and the values of x can be measured accurately.

The forms of the present solutions, while providing an alternative to estimating numerically the values of a_2/a_1 in the vicinity of the caustic, also give an indication as to what the wave profiles look like in this region in a general situation. From the forms of these solutions and on a consideration of the characteristics of their parameters, it is apparent that the highest wave will always occur at a short distance from the caustic and possess a configuration similar to a single progressive sinusoidal wave instead of having the features of a short wave riding on a long wave. Consequently, in storm conditions, this individual wave results in a deep trough preceding a steeper forward face, which is consistent with the description of freak waves given by Mallory (1974). The exact configuration and location of this highest individual wave will surely be subject to modification by the nonlinear effects, but according to Smith (1976) and Peregrine & Smith (1979), its near-linear solution resembling the linear Airy function solution with a marked shift of the phase and an enhancement of the asymmetry of the wave profile, can be stable. For a discussion of the finite-amplitude solutions rather than near-linear solutions, reference should be made to Peregrine & Thomas (1979).

We are deeply grateful to Professor O. M. Phillips for his invaluable advice and encouragement. One of the authors (J.-H. Shyu) was initiated and guided by Professor Phillips into the study of the present research and is greatly indebted to him. Also we are indebted to Professor Norden E. Huang for his helpful suggestions. Comments and suggestions by the referees and Professor Chiang C. Mei to improve the presentation of this work and to include a physical discussion of the present results as we did in § 8 are gratefully acknowledged. This research was initiated when Chi-Chao Tung was invited by the National Science Council of the Republic of China to visit Taiwan, and was completed with the support of the National Science Council under contract NSC 83-0209-E-124-005 and with the transportation construction funding from the Taiwan provincial government.

REFERENCES

Bretherton, F. P. & Garrett, C. J. R. 1968 Wavetrains in inhomogeneous moving media. *Proc. R. Soc. Lond.* A **302**, 529–554.

Henyey, F. S., Creamer, D. B., Dysthe, K. B., Schult, R. L. & Wright, J. A. 1988 The energy and action of small waves riding on large waves. *J. Fluid Mech.* **189**, 443–462.

Holthuijsen, L. H. & Tolman, H. L. 1991 Effects of the Gulf Stream on ocean waves. *J. Geophys. Res.* **96**, 12755–12771.

Longuet-Higgins, M. S. 1985 Accelerations in steep gravity waves. *J. Phys. Oceanogr.* **15**, 1570–1579.

Longuet-Higgins, M. S. 1987 The propagation of short surface waves on longer gravity waves. *J. Fluid Mech.* **177**, 293–306.

Longuet-Higgins, M. S. & Stewart, R. W. 1960 Changes in the form of short gravity waves on long waves and tidal currents. *J. Fluid Mech.* **8**, 565–583.

Longuet-Higgins, M. S. & Stewart, R. W. 1961 The changes in amplitude of short gravity waves on steady non-uniform currents. *J. Fluid Mech.* **10**, 529–549.

Mallory, J. K. 1974 Abnormal waves on the south east coast of South Africa. *Intl Hydrog. Rev.* **51**, 99–129.

Mei, C. C. 1983 *The Applied Dynamics of Ocean Surface Waves.* Interscience.

Peregrine, D. H. 1976 Interaction of water waves and currents. *Adv. Appl. Mech.* **16**, 9–117.

Peregrine, D. H. & Smith, R. 1979 Nonlinear effects upon waves near caustics. *Phil. Trans R. Soc. Lond.* A **292**, 341–370.

Peregrine, D. H. & Thomas, G. P. 1979 Finite-amplitude deep-water waves on currents. *Phil. Trans R. Soc. Lond.* A **292**, 371–390.

Phillips, O. M. 1977 *The Dynamics of the Upper Ocean*, 2nd Edn. Cambridge University Press.

Phillips, O. M. 1981 The dispersion of short wavelets in the presence of a dominant long wave. *J. Fluid Mech.* **107**, 465–485.

Phillips, O. M. 1988 Remote sensing of the sea surface. *Ann. Rev. Fluid Mech.* **20**, 89–109.

Phillips, O. M., Gu, D. & Donelan, M. 1993*a* Expected structure of extreme waves in a Gaussian sea. Part I: Theory and SWADE buoy measurements. *J. Phys. Oceanogr.* **23**, 992–1000.

Phillips, O. M., Gu, D. & Walsh, E. J. 1993*b* On the expected structure of extreme waves in a Gaussian sea. Part II: SWADE Scanning Radar Altimeter Measurements. *J. Phys. Oceanogr.* **23**, 2297–2309.

Shyu, J. H. & Phillips, O. M. 1990 The blockage of gravity and capillary waves by longer waves and currents. *J. Fluid Mech.* **217**, 115–141.

Smith, R. 1975 The reflection of short gravity waves on a non-uniform current. *Math. Proc. Camb. Phil. Soc.* **78**, 517–525.

Smith, R. 1976 Giant waves. *J. Fluid Mech.* **77**, 417–431.

Trulsen, K. & Mei, C. C. 1993 Double reflection of capillary/gravity waves by a non-uniform current: a boundary-layer theory. *J. Fluid Mech.* **251**, 239–271.

Tung, C. C. & Shyu, J. H. 1992 Wave spectrum in adverse current. *Proc. 2nd Intl Offshore Polar Engng Conf.*, pp. 119–123, San Francisco. *Intl Soc. Offshore Polar Engng.*

Turrittin, H. L. 1952 Asymptotic expansions of solutions of systems of ordinary differential equations. In *Contributions to the Theory of Nonlinear Oscillations II.* Annals of Math Studies, vol. 29, pp. 81–116, Princeton University Press.

Wasow, W. 1985 *Linear Turning Point Theory.* Springer.

White, B. S. & Fornberg, B. 1998 On the chance of freak waves at sea. *J. Fluid Mech.* **355**, 113–138.

Whitham, G. B. 1965 A general approach to linear and nonlinear dispersive waves using a Lagrangian. *J. Fluid Mech.* **22**, 273–283.

Whitham, G. B. 1974 *Linear and Nonlinear Waves.* John Wiley & Sons.